applied sciences

MDPI

Article

Computational and Experimental Study on Molecular Structure of Benzo[*g*]pyrimido[4,5-*b*]quinoline Derivatives: Preference of Linear over the Angular Isomer

Jorge Trilleras [1,*], Dency José Pacheco [1], Alfredo Pérez-Gamboa [1], Jairo Quiroga [2], Alejandro Ortiz [2], Jaime Gálvez [3], Manuel Nogueras [4] and Justo Cobo [4]

1 Grupo/Semillero de Investigación en Compuestos Heterocíclicos, Programa de Química, Facultad de Ciencias Básicas, Universidad del Atlántico, Puerto Colombia, Atlántico, Colombia; dencypacheco@mail.uniatlantico.edu.co (D.J.P.); alfredoperez@mail.uniatlantico.edu.co (A.P.-G.)

2 Grupo de Investigación de Compuestos Heterocíclicos, Departamento de Química, Universidad del Valle, A. A 25360, Cali, Colombia; jairo.quiroga@correounivalle.edu.co (J.Q.); alejandro.ortiz@correounivalle.edu.co (A.O.)

3 Centro Nacional de Asistencia Técnica a la Industria (Centro—ASTIN)—SENA, Complejo Salomia, Cali, Colombia; jaimegalvez.n@gmail.com

4 Departamento de Química Inorgánica y Orgánica, Universidad de Jaén, 23071 Jaén, Spain; mmontiel@ujaen.es (M.N.); jcobo@ujaen.es (J.C.)

* Correspondence: jorgetrilleras@mail.uniatlantico.edu.co; Tel.: +57-5-385-22-66 (ext. 1161)

Received: 22 August 2017; Accepted: 16 September 2017; Published: 21 September 2017

Abstract: A series of 5-aryl-2-methylthio-5,12-dihydrobenzo[*g*]pyrimido[4,5-*b*]quinoline-4,6,11(3*H*)-trione was synthesized through an environmental friendly multicomponent methodology and characterized with FT-IR (Fourier Transform infrared spectroscopy), ^{1}H NMR (Nuclear Magnetic Resonance), ^{13}C NMR and GC-MS (gas chromatography-mass spectrometry). The 5-(4-methoxyphenyl)-2-methylthio-5,12-dihydrobenzo[*g*]pyrimido[4,5-*b*]quinoline-4,6,11(3*H*)-trione **4c** compound was characterized by X-ray single crystal diffraction. The geometry of **4c** has been fully optimized using DFT (Density functional theory), B3LYP functional and 6-31G(d,p) basis set, thus establishing the ground state energy and thermodynamic features for the mentioned compound, which are in accordance with the experimental data and the crystal structure. The experimental results reveal a strong preference for the regioselective formation of **4c** linear four fused rings over the angular four fused and suggest a possible kinetic control in product formation.

Keywords: DFT analysis; MCR's; MW irradiation; one-pot reactions; quinoline derivatives

1. Introduction

The use of environmental friendly procedures is nowadays a standard tool in synthetic applications because of their benefits both in chemistry and environmental point of views. In this sense, reactions assisted by microwave (MW) radiation are well known because of their advantages over conventional methods, becoming an important and almost regular methodology for the synthesis of organic compounds [1–8]. On the other hand, multicomponent reaction (MCR), most running with atom economy, offer convenient procedures for the introduction of structural diversity of heterocyclic compounds which are prepared by a straightforward manner, in a single synthetic step [9–17]. Combining the advantages of MCR with those of microwave assisted organic synthesis under solvent-free conditions provides fast and efficient methods for the synthesis of heterocyclic systems, which are among the most common scaffolds in compounds with diverse applications.

Quinoline derivatives are synthetic targets because they exhibit a wide range of biological and pharmacological activities [18–23]. Compared with other derivatives that exhibit high fluorescence, quinolone derivatives are among the best candidates in the design of electroluminescent materials [24,25]. Its fusion with other interesting heterocyclic nucleus such as pyrimidine have afforded systems with high usefulness, such the pyrimido[4,5-*b*]quinoline, which have been synthesized by diverse procedures, involving condensation and cyclocondensation reactions [26–34].

Our research group has made great efforts to develop synthetic strategies to obtain highly functionalized heterocycles [13,14,23,27–29,35,36]. In this sense, we have recently reported about simple and environmental friendly MCR one-pot procedures for the synthesis of heterofused-quinolines such as: pyrazolo[3,4-*b*]quinolindiones [23], prepared by MW assisted synthesis under solvent-free/catalyst-free conditions, or pyrimido[4,5-*b*]quinolindiones [36] by heating in ethanol. In these reactions, also reported by other researches, the dihydroderivatives are obtained as final products (Scheme 1) [37,38].

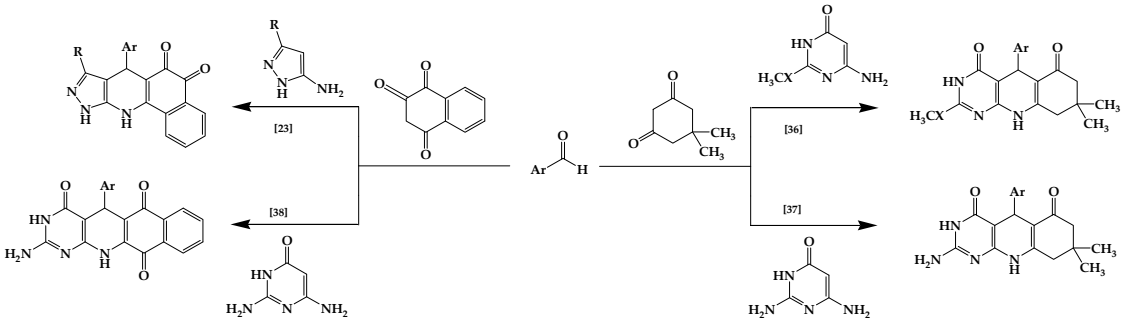

Scheme 1. Heterofused-quinoline derivatives synthesized via multicomponent reaction (MCR) procedures.

Continuing with our studies for the synthesis of aza-heterocycles, we have decided to investigate the MCR of 6-aminopyrimidin-4-ones **1**, naphthalene-1,2,4(3*H*)-trione **2** and aromatic aldehydes **3** under MW irradiation and solvent-free/catalyst free conditions in order to obtain benzopyrimidoquinolines, and so providing results for a comparative analysis with previous reported experiments [39] and the better knowledge of the reaction type involved in the formation of carbon–carbon bonds [40,41].

2. Materials and Methods

2.1. Materials and Methods

All reagents used in this work were purchased commercially without further purification. Identifications of compounds and measurements of properties were carried out by general procedures employing the following equipment: Microwave irradiation was carried out with microwave oven CEM Discover (CEM Corporation, Matthews, NC, USA) with controlled power and temperature. Melting points were determined in a Büchi Melting Point Apparatus (BUCHI Latinoamérica, Valinhos, SP, Brasil) and are reported without any corrections. The ^{1}H and ^{13}C NMR (Nuclear Magnetic Resonance) spectra were measured at RT (Room Temperature) on a Bruker Avance 400 spectrometer (Bruker, Rheinstetten, Germany) operating at 400 and 100 MHz, respectively, and using.

Dimethyl Sulfoxide deuterated (DMSO-d_6) as solvent and tetramethylsilane (TMS) as internal standard. The mass-spectra were scanned on a Hewlett Packard HP Engine-5989 spectrometer (Hewlett Packard, Palo Alto, CA, USA), equipped with a direct inlet probe which was operating at 70 eV. Elemental analyses were obtained using a LECO CHNS-900 elemental analyzer (LECO Corporation, Saint Joseph, MI, USA).

2.2. Synthesis

General Procedure for the MCR of Compounds **4a–q**

The mixture of 6-aminopyrimidin-4-one **1** (1 mmol), naphthalene-1,2,4(3*H*)-trione **2** (1 mmol) and aldehyde **3** (1 mmol), were irradiated for 5–9 min and 200 °C under solvent-free conditions. Upon completion, monitored by thin-layer chromatography (TLC), the reaction mixture was cooled to room temperature. The solid was further purified by recrystallization from EtOH (95%).

2-methylthio-5-phenyl-5,12-dihydrobenzo[g]pyrimido[4,5-b]quinoline-4,6,11(3H)-trione (**4a**). 80%. m.p. > 300 °C. IR (KBr, υ cm^{-1}), 3398 (N-H st), 2689 (CH_3 st), 1652, 1630 (C=O st). ^{1}H NMR (400 MHz, DMSO-d_6) δ (ppm): 2.55 (s, 3H, SCH_3), 5.25 (s, 1H, CH), 7.11 (t, *J* = 6.78 Hz, 1H, Hp), 7.21 (t, *J* = 7.28 Hz, 2H, Hm), 7.30 (d, *J* = 7.78 Hz, 2H, H*o*), 7.76–7.84 (m, 2H, H8, H9), 7.90 (d, *J* = 7.28 Hz, 1H, H7), 8.03 (d, *J* = 7.03 Hz, 1H, H10), 9.60 (s, 1H, NH), 12.49 (s, 1H, NH). ^{13}C NMR δ (ppm): 12.7 (SCH_3), 54.3 (C5), 117.4 (C4a), 124.5 (Cp), 125.3 (C*o*), 125.6 (C10), 127.3 (C*m*), 127.9 (C7), 130.3, 131.8 (C10a), 133.2 (C8), 134.6 (C9), 139.3 (C5a), 145.0 (Ci), 179.1 (C=O), 181.6 (C=O). MS: (70 eV) *m*/*z* = 401 (16, M^+), 325 (19), 324 (100), 276 (13). Anal. Calcd. for $C_{22}H_{15}N_3O_3S$ C, 65.82; H, 3.77; N, 10.47; found C, 65.85; H, 3.80; N, 10.45.

2-methylthio-5-(4-methylphenyl)-5,12-dihydrobenzo[g]pyrimido[4,5-b]quinoline-4,6,11(3H)-trione (**4b**). 80%. m.p. > 300 °C (dec). IR (KBr, υ cm^{-1}), 3395 (N-H st), 2929 (CH_3 st), 1651 (C=O st). ^{1}H NMR (400 MHz, DMSO-d_6) δ (ppm): 2.18 (s, 3H, CH_3), 2.55 (s, 3H, SCH_3), 5.21 (s, 1H, CH), 7.00 (d, *J* = 8.03 Hz, 2H, Hm), 7.16 (d, *J* = 8.03 Hz, 2H, H*o*), 7.77–7.84 (m, 2H, H8, H9), 7.90 (d, *J* = 7.53 Hz, 1H, H7), 8.02 (d, *J* = 7.03 Hz, 1H, H10), 9.58 (s, 1H, NH), 12.51 (s, 1H, NH). ^{13}C NMR δ (ppm): 12.7 (*p*-CH_3), 20.5 (SCH_3), 34.1 (C5), 117.7 (C4a), 125.6 (C10), 125.9 (C7), 127.7 (C*o*), 128.7 (C*m*), 130.3 (C6a), 131.9 (C10a), 133.3 (C8), 134.8 (C9), 135.6 (C2), 139.2 (C5a), 142.2 (C*i*), 179.2 (C=O), 181.7 (C=O). MS: (70 eV) *m*/*z* (%) = 415 (30, M^+), 324 (100), 276 (14). Anal. Calcd. for $C_{23}H_{17}N_3O_3S$ C, 66.49; H, 4.12; N, 10.11; found C, 66.48; H, 4.13; N, 10.14.

5-(4-methoxyphenyl)-2-methylthio-5,12-dihydrobenzo[g]pyrimido[4,5-b]quinoline-4,6,11(3H)-trione (**4c**). Yellow crystalline solid, 80%. m.p. > 300 °C (dec). IR (KBr, υ cm^{-1}), 3272 (N-H st), 2841 (CH_3 st), 1674, 1650 (C=O st). ^{1}H NMR (400 MHz, DMSO-d_6) δ (ppm): 2.55 (s, 3H, SCH_3), 3.65 (s, 3H, OCH_3), 5.18 (s, 1H, H5), 6.76 (d, *J* = 8.79 Hz, 2H, H*o*), 7.18 (d, *J* = 8.79 Hz, 2H, H*m*), 7.77–7.85 (m, 2H, H8, H9), 7.90 (d, *J* = 7.53 Hz,1H, H7), 8.02 (d, *J* =7.03 Hz, 1H, H10), 9.60 (s, 1H, H12), 12.52 (s, 1H, H3). ^{13}C NMR δ (ppm): 12.7 (SCH_3), 34.0 (OCH_3), 55.0 (C5), 114.0 (C*o*), 129.0 (C*p*), 158.0 (C=O). MS: (70 eV) *m*/*z* = 431 (61, M^+), 325 (19), 324 (100), 276 (18), 248 (12). Anal. Calcd. for $C_{23}H_{17}N_3O_4S$ C, 64.03; H, 3.97; N, 9.74; found C, 64.02; H, 4.01; N, 9.78.

2-methylthio-5-(3,4,5-trimethoxyphenyl)-5,12-dihydrobenzo[g]pyrimido[4,5-b]quinoline-4,6,11(3H)-trione (**4d**). 80%. m.p. 265 °C. IR (KBr, υ cm^{-1}), 3264 (N-H st), 2933 (CH3 st), 1656 (C=O st). ^{1}H NMR (400 MHz, DMSO-d_6) δ (ppm): 2.55 (s, 3H, SCH_3), 3.58 (s, 3H, OCH_3), 3.67 (s, 6H, OCH_3), 5.22 (s, 1H, CH), 6.57 (s, 2H), 7.77–7.85 (m, 2H, H9, H8), 7.93 (d, *J* = 8.53 Hz, 1H, H7), 8.03 (d, *J* = 8.78 Hz, 1H, H10), 9.49 (s, 1H, NH), 12.48 (s, 1H, NH). ^{13}C NMR δ (ppm): 12.5 (SCH_3), 34.5 (C5), 55.7 (OCH_3), 59.6 (OCH_3), 105.2 (C*o*), 125.4 (C7), 125.7 (C10), 133.0 (C8), 134.5 (C9), 135.6, 136.3 (C5a), 139.2, 140.3 (C*i*), 152.4 (C11a), 178.9 (C=O), 181.5 (C=O). MS: (70 eV) *m*/*z* (%) = 491 (48, M^+), 460 (17), 325 (19), 324 (100), 276 (18). Anal. Calcd. for $C_{25}H_{21}N_3O_6S$ C, 61.09; H, 4.31; N, 8.55; found C, 61.12; H, 4.30; N, 8.58.

2-methylthio-5-(2-thienyl)-5,12-dihydrobenzo[g]pyrimido[4,5-b]quinoline-4,6,11(3H)-trione (**4e**). 70%. m.p. > 300 °C. IR (KBr, υ cm^{-1}), 3384 (N-H st), 2969 (CH_3 st), 1655 (C=O st). ^{1}H NMR (400 MHz, DMSO-d_6) δ (ppm): 2.55 (s, 3H, SCH_3), 5.53 (s, 1H, CH), 6.81–6.85 (m, 2H, Hetaryl), 7.25 (d, *J* = 6.28 Hz, 1H, Hetaryl) 7.77–7.86 (m, 2H, H9, H8), 7.97 (d, *J* = 8.53 Hz, 1H, H7), 8.04 (d, *J* = 8.53 Hz, 1H, H10), 9.86 (s, 1H, NH), 12.64 (s, 1H, NH). ^{13}C NMR δ (ppm): 12.7 (SCH_3), 29.1 (CH), 116.6 (C4a), 124.3 (CH, Hetaryl), 124.5 (CH, Hetaryl), 125.7 (C10), 126.0 (CH, Hetaryl), 126.7 (C7), 130.3 (C6a), 131.7 (C10a), 133.3 (C8), 134.8 (C9), 138.9 (C5a), 148.0 (C2), 179.1 (C=O), 181.5 (C=O). MS: (70 eV) *m*/*z* (%) = 407 (100, M^+), 392 (11), 346 (18), 324 (59), 276 (18). Anal. Calcd. for $C_{20}H_{13}N_3O_3S_2$ C, 58.95; H, 3.22; N, 10.31; found C, 58.99; H, 3.25; N, 10.34.

5-(4-fluorophenyl)-2-methylthio-5,12-dihydrobenzo[g]pyrimido[4,5-b]quinoline-4,6,11(3H)-trione (**4f**). 70%. m.p. > 300 °C. IR (KBr, υ cm^{-1}), 3337 (NH st), 1656 (C=O st). ^{1}H NMR (400 MHz, DMSO-d_6) δ (ppm): 2.56 (s, 3H, SCH_3), 5.25 (s, 1H, H5), 7.03 (t, *J* = 8.79 Hz, 2H, H*o*), 7.34 (d, *J* = 7.03 Hz, 2H, H*m*), 7.79–7.83 (m, 2H, H8, H9), 7.90 (d, *J* = 6.78 Hz, 1H, H7), 8.03 (d, *J* = 7.28 Hz, 1H, H10), 9.64 (s, 1H, NH), 12.53 (s, 1H, NH). ^{13}C NMR δ (ppm): 12.8 (SCH_3), 35.7 (C5), 114.8 (C4a), 124.8 (C10), 128.6 (C7), 129.4 (C*o*), 129.5 (C*m*), 131.1 (C8), 134.6 (C9), 141.2 (C*i*), 145.5, 162.3, 178.6 (C=O). MS: (70 eV) *m*/*z* (%) = 419 (84, M^+), 417, (25), 474 (50), 324 (100). Anal. Calcd. for $C_{22}H_{14}FN_3O_3S$ C, 63.00; H, 3.36; N, 10.02; found C, 63.04; H, 3.34; N, 10.05.

5-(4-chlorophenyl)-2-methylthio-5,12-dihydrobenzo[g]pyrimido[4,5-b]quinoline-4,6,11(3H)-trione (**4g**). 80%. m.p. > 300 °C. IR (KBr, υ cm^{-1}), 3367 (NH st), 2684 (CH_3 st), 1652, 1626 (C=O st). ^{1}H NMR (400 MHz, DMSO-d_6) δ (ppm): 2.55 (s, 3H, SCH_3), 5.23 (s, 1H, H5), 7.26 (d, *J* = 8.54 Hz, 2H, H*o*), 7.32 (d, *J* = 8.54 Hz, 2H, H*m*), 7.79–7.82 (m, 2H, H8, H9), 7.90 (d, *J* = 7.03 Hz, 1H, H7), 8.03 (d, *J* = 7.03 Hz, 1H, H10), 9.66 (s, 1H, NH), 12.53 (s, 1H, NH). ^{13}C NMR δ (ppm): 12.7 (SCH_3), 34.3 (C5), 125.6 (C10), 125.9 (C7), 128.1 (C*o*), 129.7 (C*m*), 130.4 (C6a), 131.8 (C10a), 133.3, 134.7 (C9), 139.4 (C5a), 143.9 (C*i*), 178.5 (C4), 179.2 (C=O), 181.6 (C=O). MS: (70 eV) *m*/*z* (%) = 437 (6, M^{+2}), 436 (5.7, M^{+1}), 435 (15, M^+), 326 (6), 325 (18), 324 (100), 276 (13). Anal. Calcd. for $C_{22}H_{14}ClN_3O_3S$ C, 60.62; H, 3.24; N, 9.64; found C, 60.64; H, 3.22; N, 9.68.

5-(4-bromophenyl)-2-methylthio-5,12-dihydrobenzo[g]pyrimido[4,5-b]quinoline-4,6,11(3H)-trione (**4h**). 80%. m.p. > 300 °C. IR (KBr, υ cm^{-1}), 3369 (NH st), 1658 (C=O st). ^{1}H NMR (400 MHz, DMSO-d_6) δ (ppm): 2.56 (s, 3H, SCH_3), 5.33 (s, 1H, H5), 7.54 (d, *J* = 8.28 Hz, 2H, H*o*), 7.58 (d, *J* = 8.28 Hz, 2H, H*m*), 7.77–7.82 (m, 2H, H8, H9), 7.89 (d, 1H, *J* = 7.27 Hz, H7), 8.03 (d, 1H, *J* = 7.03 Hz, H10), 9.72 (s, 1H, NH), 12.55 (s, 1H, NH). ^{13}C NMR δ (ppm): 12.7 (SCH_3), 35.0 (C5), 116.5 (C5a), 125.0, 125.6 (C10), 125.9 (C7), 127.8 (C*o*), 129.5 (C*m*), 131.7 (C10a), 133.2 (C8), 134.7 (C9), 139.7 (C*i*), 149.3 (C2), 162.2, 178.9 (C4), 179.0 (C=O), 181.5 (C=O). MS: (70 eV) *m*/*z* (%) = 469 (17), 467 (8), 325 (19), 324 (100), 276 (14). Anal. Calcd. for $C_{22}H_{14}BrN_3O_3S$ C, 55.01; H, 2.94; N, 8.75; found C, 55.04; H, 2.98 N, 8.72.

3-methyl-2-(methylthio)-5-phenyl-5,12-dihydrobenzo[g]pyrimido[4,5-b]quinoline-4,6,11(3H)-trione (**4i**). Red solid. 81%. m.p. 277 °C. IR (KBr, υ cm^{-1}), 3227 (N-H st), 1647 (C=O, st), 1522 (C=C, st). ^{1}H NMR (400 MHz, DMSO-d_6) δ (ppm): 2.62 (s, 3H, SCH_3), 3.31 (s, 3H, NCH_3), 5.24 (s, 1H. CH) 7.10 (t, *J* = 7.03 Hz, 1H, H*p*), 7.20 (t, *J* = 7.53 Hz, 2H, H*m*), 7.29 (d, *J* = 7.28 Hz, 2H, H*o*), 7.70–7.81 (m, 2H, H9, H8), 7.87 (d, *J* = 7.53 Hz, 1H, H7), 8.01 (d, *J* = 7.28 Hz, 1H, H10), 9.68 (s, 1H, NH). ^{13}C NMR δ (ppm): 14.4 (SCH_3), 30.0 (NCH_3), 35.3 (C5), 117.4 (C4a), 125.6 (C10), 125.8 (C7), 126.4 (C*p*), 128.0 (C*o*), 128.6 (C*m*), 130.3 (C6a), 131.8 (C10a), 133.2 (C8), 134.7 (C9), 139.2 (C5a), 145.0 (C*i*), 149.7 (C2), 160.2 (C4, C=O), 161.6 (C12a), 179.1 (C=O), 181.5 (C=O). MS: (70 eV) *m*/*z* (%) = 414 (11, M^+), 337 (100). Anal. Calcd. for $C_{23}H_{17}N_3O_3S$ C, 66.49; H, 4.12; N, 10.11; found C, 66.47; H, 4.15; N, 10.12.

3-methyl-2-(methylthio)-5-(4-methylphenyl)-5,12-dihydrobenzo[g]pyrimido[4,5-b]quinoline-4,6,11(3H)-trione (**4j**). Red solid. 75 %. m.p. 280 °C. IR (KBr, υ cm^{-1}), 3234 (NH st), 1650 (C=0 st), (1521 C=C st). ^{1}H NMR (400 MHz, DMSO-d_6) δ (ppm): 2.18 (s, 3H, *p*-CH_3), 2.63 (s, 3H, SCH_3), 2.75 (s, 3H, NCH_3), 5.22 (s, 1H, H5), 7.02 (d, *J* = 8.03 Hz, 2H, H*m*), 7.17 (d, *J* = 8.03, 2H, H*o*), 7.79–7.83 (m, 2H, H8, H9), 7.90 (d, *J* = 7.28 Hz, 1H, H7), 8.03 (d, *J* = 7.28 Hz, 1H, H-10), 9.72 (s, 1H, NH). ^{13}C NMR δ (ppm): 14.4 (*p*-CH_3), 20.5 (SCH_3), 29.8 (NCH_3), 34.9 (C5), 117.6 (C4a), 125.6 (C10), 125.8 (C7), 127.8 (C*o*), 128.6 (C*m*), 130.3 (C6a), 131.8 (C10a), 133.2 (C8), 134.7 (C9), 135.5 (C11a), 139.1 (C5a), 142.1 (C*i*), 149.7 (C2), 160.2 (C=O), 161.4 (C12a), 179.2 (C=O), 181.6 (C=O). MS: (70 eV) *m*/*z* (%) = 429 (22, M^+), 337 (100). Anal. Calcd. for $C_{24}H_{19}N_3O_3S$ C, 67.12; H, 4.46; N, 9.78; found C, 67.15; H, 4.45; N, 9.76.

3-methyl-5-(4-methoxyphenyl)-2-methylthio-5,12-dihydrobenzo[g]pyrimido[4,5-b]quinoline-4,6,11(3H)-trione (**4k**). Red solid. 70%. m.p. 282 °C. IR (KBr, υ cm^{-1}), 3222 (NH st), 1647 (C=O st). ^{1}H NMR (400 MHz, DMSO-d_6) δ (ppm): 2.63 (s, 3H, SCH_3), 3.32 (s, 3H, NCH_3), 3.84 (s, 3H, OCH_3), 5.21 (s, 1H, H5), 6.77 (d, *J* = 8.79 Hz, 2H, H*o*), 7.21 (d, *J* = 8.53 Hz, 2H, H*m*), 7.78–7.82 (m, 2H, H8, H9), 7.89 (d, *J* = 8.54 Hz, 1H, H7), 8.03 (d, *J* = 8.53 Hz, 1H, H10), 9.66 (s, 1H, NH). ^{13}C NMR δ (ppm): 14.4 (SCH_3), 29.9 (NCH_3),

34.4 (C5), 54.9 (OCH_3), 113.5 (C*o*), 117.7 (C4a), 125.6 (C10), 128.8 (C*m*), 130.3 (C6a), 131.8 (C*i*), 133.1 (C7), 134.7 (C9), 137.3 (C10a), 138.9 (C5a), 149.6 (C2), 157.8 (C2), 160.2 (C=O), 161.4 (C12a). MS: (70 eV) *m*/*z* (%) = 445 (45, M^+), 337 (100). Anal. Calcd. for $C_{24}H_{19}N_3O_4S$ C, 64.71; H, 4.30; N, 9.43; found C, 64.75; H, 4.27; N, 9.45.

3-methyl-2-(methylthio)-5-(3,4,5-trimethoxyphenyl)-5,12-dihydrobenzo[g]pyrimido[4,5-b]quinoline-4,6,11(3H)-trione (**4l**). Brown solid. 80%. m.p. 263 °C. IR (KBr, υ cm^{-1}), 3243 (NH st), 1648 (C=O st). ^{1}H NMR (400 MHz, DMSO-d_6) δ (ppm): 2.62 (s, 3H, SCH_3), 3.33 (s, 3H, NCH_3), 3.56 (s, 3H, OCH_3), 3.67 (s, 6H, OCH_3), 5.21 (s, 1H, H5), 6.57 (s, 2H, H*o*) 7.78–7.82 (m, 2H, H8, H9), 7.91 (d, *J* = 7.28 Hz, 1H, H7), 8.03 (d, *J* = 7.28 Hz, 1H, H10), 9.60 (s, 1H, NH). ^{13}C NMR δ (ppm): 14.4 (SCH_3), 29.9 (NCH_3), 35.6 (C5), 55.8 (OCH_3), 59.7 (OCH_3), 105.6 (C*o*), 117.1 (C4a), 125.6 (C7), 125.8 (C10), 130.4 (C6a), 131.8 (C10a), 133.1 (C8), 134.6 (C9), 136.5 (C5a), 140.6 (C*i*), 149.7 (C2), 152.5 (C11a), 161.5 (C12a), 179.1 (C=O), 181.6 (C=O). MS: (70 eV) *m*/*z* (%) = 505 (76, M^+), 474 (15), 337 (100). Anal. Calcd. for $C_{26}H_{23}N_3O_6S$ C, 61.77; H, 4.59; N, 8.31; found C, 61.79; H, 4.62; N, 8.34.

3-methyl-2-(methylthio)-5-(4-trifluoromethylphenyl)-5,12-dihydrobenzo[g]pyrimido[4,5-b]quinoline-4,6,11(3H)-trione (**4m**). Red solid. 75%. m.p. >300 °C. IR (KBr, υ cm^{-1}), 3447 (NH st), 1687 (C=O st), 1519 (C=C st). ^{1}H NMR (400 MHz, DMSO-d_6) δ (ppm): 2.74 (s, 3H, SCH_3), 2.88 (s, 3H, NCH_3), 5.33 (s, 1H, H5), 7.39 (d, *J* = 7.03 Hz, 1H, H7), 7.56 (d, *J* = 7.06 Hz, 2H, H*o*), 7.72–7.74 (d, *J* = 7.03 Hz, 2H, H*m*), 7.80 (t, 1H, H8), 7.89 (t, 1H, H9), 8.03 (d, *J* = 7.03 Hz, 1H, H10), 9.88 (s, 1H, NH). ^{13}C NMR δ (ppm): 14.5 (SCH_3), 29.9 (NCH_3), 35.7 (C5), 99.5 (C4a), 111.6 (C5a), 127.0 (C10), 127.3 (C*o*), 128.0 (C7), 128.9 (C*m*), 133.2 (C8), 135.4 (C9), 139.7 (C*i*), 149.8 (C2), 157.3, 159.2 (C6a), 160.2 (C=O), 166.1 (C12a), 178.3 (C=O), 198.50 (C6). MS: (70 eV) *m*/*z* (%) = 480 (18, M^+), 337 (100), 437 (40). Anal. Calcd. for $C_{24}H_{16}F_3N_3O_3S$ C, 59.62; H, 3.34; N, 8.69; found C, 59.65; H, 3.30; N, 8.73.

5-(benzo[d][1,3]dioxol-6-yl)-3-methyl-2-methylthio-5,12-dihydrobenzo[g]pyrimido[4,5-b]quinoline-4,6,11(3H)-trione (**4n**). Red solid. 75%. m.p. 254 °C. IR (KBr, υ cm^{-1}), 3225 (NH st), 1647 (C=O st), 1519 (C=C st). ^{1}H NMR (400 MHz, DMSO-d_6) δ (ppm): 2.63 (s, 3H, SCH_3), 3.34 (s, 3H, NCH_3), 5.19 (s, 1H, H5), 5.91 (s, 2H, CH_2), 6.74 (d, *J* = 6.79 Hz, 2H, aryl), 6.86 (s, 1H, aryl), 7.78–7.84 (m, 2H, H8, H9), 7.91 (d, *J* = 7.89 Hz, 1H, H7), 8.03 (d, *J* = 8.02 Hz, 1H, H10), 9.72 (s, 1H, NH). ^{13}C NMR δ (ppm): 14.45 (SCH_3), 29.9 (NCH_3), 35.0 (C5), 100.7 (CH_2), 107.8, 108.6 (C2′-C6′), 117.3 (C4a), 121.0 (C5′), 125.6 (C10), 125.9 (C7), 130.4 (C6a), 131.8 (C10a), 133.2 (C8), 134.7 (C9), 139.1 (C5a), 145.8 (C*i*), 146.9 (C11a), 149.6 (C2), 160.3 (C=O), 161.6 (C12a), 179.2 (C=O), 181.6 (C6). MS: (70 eV) *m*/*z* (%) = 458 (38, M^+), 337 (100). Anal. Calcd for $C_{24}H_{17}N_3O_5S$ C, 62.74; H, 3.73; N, 9.15; found C, 62.71; H, 3.71; N, 9.18.

5-(4-fluorophenyl)-3-methyl-2-methylthio-5,12-dihydrobenzo[g]pyrimido[4,5-b]quinoline-4,6,11(3H)-trione (**4o**). Red solid. 74%. m.p. 276 °C. IR (KBr, υ cm^{-1}), 3237 (NH st), 1646 (C=O st). ^{1}H NMR (400 MHz, DMSO-d_6) δ (ppm): 2.61 (s, 3H, SCH_3), 3.30 (s, 3H, NCH_3), 5.22 (s, 1H, H5), 7.01 (d, *J* = 7.30 Hz, 2H, H*o*), 7.32 (t, *J* = 7.30 Hz, 2H, H*m*), 7.77–7.82 (m, 2H, H8, H9), 7.87 (d, *J* = 7.98 Hz, 1H, H7), 8.01 (d, *J* = 7.03 Hz, 1H, H10), 9.73 (s, 1H, NH). ^{13}C NMR δ (ppm): 14.4 (SCH_3), 29.9 (NCH_3), 34.8 (C5), 114.6 (C4a), 114.8 (C6a), 117.1 (C10a), 125.6 (C10), 125.9 (C7), 129.8 (C*o*), 130.3 (C*m*), 131.7 (C11a), 133.2 (C8), 134.7 (C9), 139.3 (C*i*), 149.8 (C2), 179.1 (C=O), 181.5 (C=O). MS: (70 eV) *m*/*z* (%) = 441 (7, M^+), 432 (22), 430 (42), 387 (75), 337 (100). Anal. Calcd. for $C_{23}H_{16}FN_3O_3S$ C, 63.73; H, 3.72; N, 9.69; found C, 63.77; H, 3.76; N, 9.70.

5-(4-chlorophenyl)-3-methyl-2-methylthio-5,12-dihydrobenzo[g]pyrimido[4,5-b]quinoline-4,6,11(3H)-trione (**4p**). Red solid. 71%. m.p. 283 °C. IR (KBr, υ cm^{-1}), 3233 (NH st), 1648 (C=O st). ^{1}H NMR (400 MHz, DMSO-d_6) δ (ppm): 2.62 (s, 3H, SCH_3), 3.31 (s, 3H, NCH_3), 5.24 (s, 1H, H5), 7.24 (d, *J* =8.28 Hz, 2H, H*o*), 7.32 (d, *J* = 8.28 Hz, 2H, H*m*), 7.78–7.82 (m, 2H, H8, H9), 7.88 (d, *J* = 7.28 Hz, 1H, H7), 8.02 (d, *J* = 7.28 Hz, 1H, H10), 9.75 (s, 1H, NH). ^{13}C NMR δ (ppm): 14.4 (SCH_3), 29.8 (NCH_3), 35.1 (C5), 116.8 (C4a), 125.6 (C10), 125.9 (C7) 127.9 (C*o*), 129.8 (C*m*), 133.2 (C8), 134.7 (C9), 139.5 (C5a), 143.9 (C*i*), 149.7 (C2), 160.2 (C4), 161.8 (C12a), 179.1 (C=O), 181.5 (C=O). MS: (70 eV) *m*/*z* (%) 448 (12, M^+), 337 (100). Anal. Calcd. for $C_{23}H_{16}ClN_3O_3S$ C, 61.40; H, 3.58; N, 9.34; found C, 61.37; H, 3.57; N, 9.33.

5-(4-bromophenyl)-3-methyl-2-methylthio-5,12-dihydrobenzo[g]pyrimido[4,5-b]quinoline-4,6,11(3H)-trione (**4q**). Red solid. 76%. m.p. 264 °C. IR (KBr, υ cm^{-1}), 3228 (NH st), 1650 (C=O st). ^{1}H NMR (400 MHz, DMSO-d_6) δ (ppm): 2.62 (s, 3H, SCH_3), 3.30 (s, 3H, NCH_3), 5.20 (s, 1H, H5), 7.25 (d, *J* = 8.29 Hz, 2H, H*o*), 7.37 (d, *J* = 8.53 Hz, 2H, H*m*), 7.77–7.81 (m, 2H, H8, H9), 7.88 (d, *J* = 7.27 Hz, 1H, H7), 8.01 (d, *J* = 8.03 Hz, 1H, H10), 9.73 (s, 1H, NH). ^{13}C NMR δ (ppm): 14.4 (SCH_3), 29.8 (NCH_3), 35.2 (C5), 99.4 (C4a), 116.7 (C5a), 119.5 (C*p*) 125.5 (C10), 125.8 (C7), 130.2 (C*o*), 130.3 (C6a), 130.9 (C*m*), 131.7 (C10a), 133.2 (C8), 134.7 (C9), 139.4 (C*i*), 144.3 (C11a), 149.7 (C2), 160.1 (C4), 161.8 (C12a), 179.0 (C=O), 181.5 (C=O). MS: (70 eV) *m*/*z* (%) = 492 (9, M^+), 337 (100). Anal. Calcd. for $C_{23}H_{16}BrN_3O_3S$ C, 55.88; H, 3.26; N, 8.50; found C, 55.91; H, 3.29; N, 8.49.

^{1}H NMR spectra and spectroscopic data for all compounds are included in the supplementary materials.

2.3. Computational Details

DFT (Density functional theory) and B3LYP/6-31G(d,p) Analysis

The 5-(4-methoxyphenyl)-2-methylthio-5,12-dihydrobenzo[*g*]pyrimido[4,5-*b*]quinoline-4,6,11(3*H*)-trione **4c** compound was optimized based on the crystal structure. The geometry has been fully optimized using DFT with the Becke three-parameter hybrid exchange and the Lee–Yang–Parr correlation density functional (B3LYP) and the Pople's split-valence 6-31G(d,p) extended basis set. The optimum structures obtained were further certified as true minima by constructing and diagonalizing the corresponding Cartesian Hessian matrix, this procedure providing also the harmonic vibrational frequencies which, after properly scaled by the recommended scaling factor 0.964, allow reliable calculations of the thermal corrections to the molecular energy. The conformational studies, natural bond orbital (NBO) and nonlinear optical (NLO) analysis on the title compound were performed; the NBO analyses were done on B3LYP/6-31+G(d,p) wave functions obtained with the B3LYP/6-31G(d,p) optimum geometries. All calculations were performed by using Gaussian 09W program package (Version A.02, Gaussian, Inc., Wallingford, CT, USA, 2009) [42].

3. Results and Discussion

3.1. Chemistry

For the preparation of benzo[*g*]pyrimido[4,5-*b*]quinolines, three-component reactions assisted by MW irradiation were carried out using as reagents 6-amino-2-(methylthio)pyri,idin-4(3*H*)-one 1, naphthalene-1,2,4(3*H*)-trione 2 and benzaldehyde 3a, in equimolar amounts. Taking as a model reaction the synthesis of 4a, we have tested several reaction conditions, combining diverse solvents (ethanol, acetic acid and ethylenglycol), temperatures and power of the microwave source in order to find the optimal conditions (Table 1). It was found that the product 4a is formed with higher yield under solvent/catalyst-free conditions, (Table 1, entry 2). The synthesis of 4a was carried out at reflux (using ethanol, acetic acid, ethylenglycol or a mixture of both) obtaining low yields and longer reaction times in contrast to MW method. When ethanol was used as the solvent by conventional heating, the desired product 4a was obtained after 2 h in low yield (30%, Table 1, entry 7). In the case of using AcOH or AcOH/Ethylenglycol mixtures moderate similar yields were obtained (45–50%, entry 8–10).

The extension of reaction times, keeping the same reaction conditions, did not lead to the formation of aromatized derivative. On the contrary, a decrease was observed in the reaction yield and double recrystallization of the crude reaction is required, first using a N,N-Dimethylformamide (DMF)-Ethanol mixture (ratio 1–9 *v*/*v*) and the isolated solid is then recrystallized from ethanol.

Considering the optimal conditions, that is, solvent/catalysis-free conditions, and in order to show the generality and scope of this protocol, we tried various aromatic aldehydes, 6-amino-2-(methylthio)pyrimidin-4(3*H*)-one and 6-amino-3-methyl-2-(methylthio)pyrimidin-4(3*H*)-one, to prepare a series of compounds **4a**–**q** (Scheme 2).

Table 1. Evaluation of the parameters of the multicomponent reaction (MCR) of compound **4a**. *

Entry	Reaction Conditions	Time (min)	Yield ** (%)
1	MW (microwave, 150 °C) solvent/catalysis-free	10	50
2	MW (200 °C) solvent/catalysis-free	5	80
3	MW (150 °C) AcOH/Ethanol (3:1)	10	50
4	MW (200 °C) AcOH/Ethanol (3:1)	5	65
5	MW (150 °C) AcOH/Ethylenglycol (3:1)	10	50
6	MW (200 °C) AcOH/Ethylenglycol (3:1)	5	70
7	Reflux, Ethanol	120	30
8	Reflux, AcOH	90	50
9	Reflux, AcOH/Ethylenglycol (3:1)	60	45
10	Reflux, AcOH/Ethylenglycol (1:3)	60	45

* Equimolar amounts of reactants (1.0 mmol). Ratio (*v*/*v*) for the solvent mixture; ** Isolated yield.

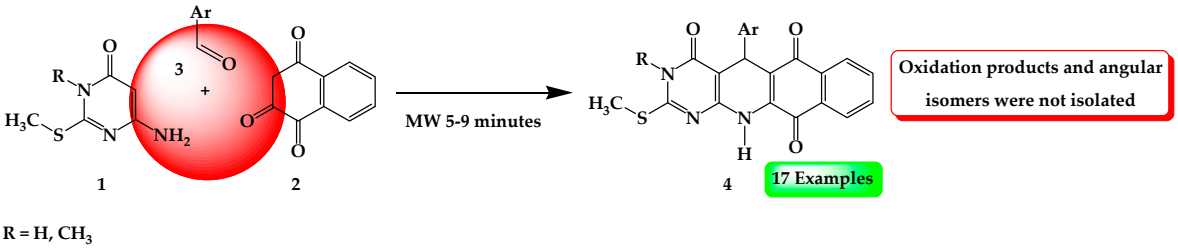

Scheme 2. Microwave (MW)-assisted synthesis of 5-aryl-2-methylthio-5,12-dihydrobenzo[*g*]pyrimido [4,5-*b*]quinoline-4,6,11(3*H*)-trione derivatives **4a–q**.

In all cases, the starting materials were completely consumed, in times ranged between 5 to 9 min, to afford the 5-aryl-2-methyltio-5,12-dihydrobenzo[*g*]pyrimido[4,5-*b*]quinoline-4,6,11(3*H*)-trione derivatives **4a–q** with high yields (70–81%) after easy work-up (Table 2).

Table 2. Results of microwave (MW)-assisted synthesis of **4a–q** compounds, in solvent/catalyst-free conditions.

Compound 4	R	Ar	Time (min)	Yield * (%)	mp (°C)
a	H	C_6H_5	5	80	>300
b[a]		*p*-CH_3-C_6H_4	5	80	>300 [a]
c[a]		*p*-OCH_3-C_6H_4	5	80	>300 [a]
d		3,4,5-*tri*-OCH_3-C_6H_2	5	80	265
e		2-Thienyl	5	70	>300
f		*p*-F-C_6H_4	5	70	>300
g		*p*-Cl-C_6H_4	5	80	>300
h		*p*-Br-C_6H_4	5	80	>300
i	CH3	C_6H_5	6	81	277
j		*p*-CH_3-C_6H_4	8	75	280
k		*p*-OCH_3-C6H4	9	70	282
l		3,4,5-*tri*-OCH_3-C_6H_2	6	80	263
m		*p*-CF_3-C_6H_4	6	75	>300
n		3,4-(OCH_2O)-C_6H_3	8	75	254
o		4-F-C_6H_4	9	74	276
p		4-Cl-C_6H_4	6	71	283
q		4-Br-C_6H_4	6	76	264

[a] Compounds which showed decomposition. * Isolated yield.

This reaction permits the use of aromatic aldehydes with electron withdrawing group (EWG) or electron releasing group (ERG), but also to 2- or/and 3-substitutedpyrimidin-4-ones with good

yields. As shown in Table 2, the difference between the yields of the compounds obtained are not significant, results suggest that the electronic nature of the substituent on aromatic aldehydes and the pyrimidin-4-ones have no significant effect on rate, yields and the course to lead to aromatization of pyridinic ring.

This protocol is a like a Mannich-type reaction, which compared with conventional methods, does not require long reaction times, and the use of flammable solvents, or expensive and toxic catalysts (ionic liquids, superacid, Brønsted acids), to obtain regioselectivelly the reaction products [40,41,43,44].

The structures of 5-aryl-2-methylthio-5,12-dihydrobenzo[*g*]pyrimido[4,5-*b*]quinoline-4,6,11(3*H*)-trione **4a–q** derivatives were elucidated from the standart spectroscopic and analytical methods (^{1}H, ^{13}C NMR, IR, mass spectra and Elemental Analysis (EA). The naphtoquinone system formed by the two non-equivalent nucleophilic center of 6-aminopyrimidinone **1** (-NH_2 group and C-5), is evidenced from ^{1}H NMR spectra. All derivatives **4a–q** showed a singlet between 5.17–5.53 ppm assigned to methine proton (stereogenic centre) and other single between 9.21–9.89 ppm corresponding to NH of the pyridine ring. All protons exhibit chemical shift signals in their respective expected region. In this reaction, two possible regioisomer could be formed depending on the carbonyl group of naphthalene-1,2,4(3*H*)-trione **2** involved in the cyclocondensation with the amino group (Figure 1).

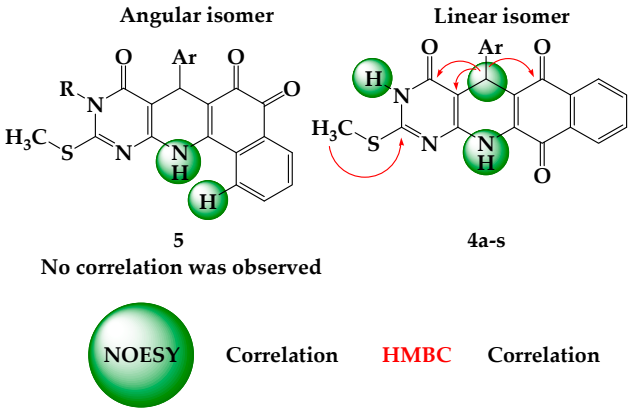

Figure 1. The NOESY (Nuclear Overhauser Effect Spectroscopy) experiment showed no correlation between NH-aromatic hydrogen. HMBC (Heteronuclear Multiple Bond Correlation) spectrum shows correlations between SCH_3/C2, C(5)H/C4, C(5)H/C4a and C(5)H/C7.

NOESY (Nuclear Overhauser Effect Spectroscopy) experiments show no correlation between the NH from dihydropyridine (DHP) ring and aromatic protons of the naphtoquinone system as expected for the non-linear derivatives **5**. It is clear that the lack of correlation is not sufficient to rule out a structure, but this is confirmed with the rest of spectroscopic analysis. In similar work, we have changed the amino-heterocyclic component (5-amino-1-NH-pyrazole by 6-amino-pyrimidinone), both bearing two non-equivalent nucleophilic center (-NH_2 group and C-4 in pyrazole or C-5 in pyrimidinone). In order to obtain pyrazolo[3,4-*b*]quinolindiones derivatives, the reaction with (1-NH)-5-aminopyrazole, which has an additional nucleophilic center lead regioselectivelly to the formation of non-linear tetracyclic dihydrocompounds. The difference between the works is the change of process regioselectivity, ortho-quinone derivatives (angular) are obtained with aminopyrazoles [23] and para-quinone derivatives (lineal) are obtained with aminopyrimidinones [37]. Now, as compared to similar work previously reported [39], the absolute configuration of the products **4** was determined by both the NMR and the X-ray analysis, showing that the linear isomer is isolated [45] including a computational study of the molecular structure of **4** compounds.

3.2. Theoretical Calculations

To unambiguously define the structures of **4**, we attempted to obtain a crystal of suitable for X-ray analysis (Figure 2). Crystal of 5-(4-methoxyphenyl)-2-methylthio-5,12-dihydrobenzo[*g*]pyrimido [4,5-*b*]quinoline-4,6,11(3*H*)-trione 4c was grown in ethanol (95%) using the slow evaporation method at room temperature (RT) [45].

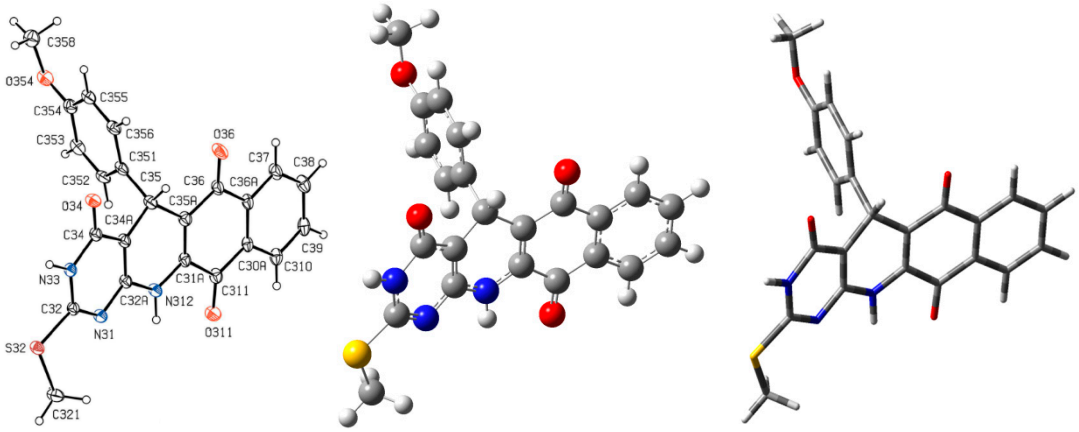

Figure 2. X-ray structure of 5-(4-methoxyphenyl)-2-methylthio-5,12-dihydrobenzo[*g*]pyrimido[4,5-*b*] quinoline-4,6,11(3*H*)-trione **4c**: (**Left**) ORTEP (Oak Ridge Thermal Ellipsoid Plot diagram), displacement ellipsoids are drawn at the 30% probability level. (**Middle**) The optimized structure with B3LYP/6-31G(d,p) level, ball and bond type. (**Right**) The optimized structure with B3LYP/6-31G(d,p) level.

In accordance with the X-ray structural analysis of 5-(4-methoxyphenyl)-2-methylthio-5,12-dihydrobenzo[*g*]pyrimido[4,5-*b*]quinoline-4,6,11(3*H*)-trione **4c**, the computational studies indicate that the dihydropyridine ring in these compounds has a boat conformation due to the presence of a sp^3 hybridized C5-atom in which the aryl ring occupies the pseudo-axial position. The orientation of the additional substituent on the C5-aryl ring (CH_3O) located on the *para*-positions with respect to the heterocyclic ring may be *syn*-orientated to the C5-H bond (synperiplanar, C5-H *sp*), or may lie above the heterocyclic ring and anti-orientated to the C5-H bond (antiperiplanar, C5-H *ap*) (Figure 3).

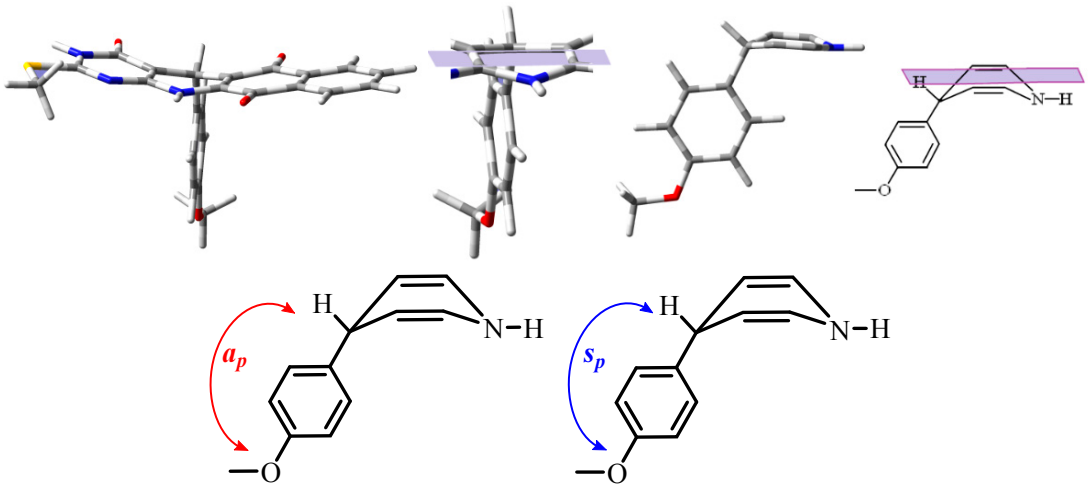

Figure 3. Conformation of the dihydropyridine ring in the structure of compound **4c**.

The optimized structures of the compound considered in the present study are illustrated in Figure 3, in which the CH_3O group has the more stable planar conformation. Structural and bonding analysis of these compounds is started by comparison of the selected bond lengths, and bond dihedral angles. Orientation of the CH_3S group with respect to the heterocyclic ring pyrimidine is denoted by a dihedral angle$\tau 1$ (N_1-C_2-S_{19}-C_{20}), inter-ring dihedral angles defining orientations of the aryl ring towards the heterocyclic ring are indicated as $\tau 2$ (C_{14}-C_5-C_{24}-C_{29}), and the inner dihedral angles of the dihydropyridine ring are denoted by $\tau 3$ (N_{12}-C_{13}-C_{14}-C_5) and $\tau 4$ (N_{12}-C_{18}-C_{15}-C_5), and dihedral angle $\tau 5$ (C_{28}-C_{27}-O_{44}-C_{45}) the 4-metoxi group the 5-aryl, which are extracted from the optimized structures of compound **4c** (Figure 3) and listed in Table 3. These orientations may influence the molecular energy content and the changes of some characteristic bond lengths, bond angles and bond dihedral angles.

Table 3. X-ray experimental analysis data and lengths, angles and dihedral angles bonds of **4c** calculated by Density functional theory (DFT) method.

Parameter			Parameter		
Bond Length (Å)	**Experimental X-ray**	**6-31G(d,p)**	**Bond Length (Å)**	**Experimental X-ray**	**6-31G(d,p)**
N_1-C_2	1.31 (4)	1.33	C_{11}-C_{17}	1.50 (4)	1.49
N_1-C_{13}	1.37 (4)	1.40	C_{11}-C_{18}	1.50 (4)	1.51
C_2-N_3	1.36 (4)	1.38	C_{11}-O_{23}	1.22 (4)	1.21
C_2-S_{19}	1.75 (3)	1.76	N_{12}-C_{13}	1.38 (4)	1.40
N_3-C_4	1.39 (4)	1.47	N_{12}-C_{18}	1.37 (4)	1.41
C_4-C_{14}	1.43 (4)	1.44	C_{13}-C_{14}	1.37 (4)	1.39
C_4-O_{21}	1.24 (4)	1.21	C_{15}-C_{18}	1.34 (4)	1.36
C_5-C_{14}	1.52 (4)	1.51	C_{16}-C_{17}	1.39 (4)	1.41
C_5-C_{15}	1.52 (4)	1.52	S_{19}-C_{20}	1.79 (3)	1.80
C_5-C_{24}	1.54 (5)	1.52	C_{24}-C_{25}	1.39 (4)	1.41
C_6-C_{15}	1.47 (4)	1.49	C_{24}-C_{29}	1.38 (5)	1.40
C_6-C_{16}	1.50 (4)	1.50	C_{25}-C_{26}	1.38 (5)	1.39
C_6-O_{22}	1.22 (4)	1.21	C_{26}-C_{27}	1.38 (5)	1.41
C_7-C_8	1.38 (4)	1.4	C_{27}-C_{28}	1.40 (5)	1.40
C_7-C_{16}	1.39 (4)	1.40	C_{27}-O_{44}	1.37 (4)	1.38
C_8-C_9	1.39 (5)	1.39	C_{28}-C_{29}	1.37 (5)	1.40
C_9-C_{10}	1.38 (5)	1.40	O_{44}-C_{45}	1.44 (4)	1.45
C_{10}-C_{17}	1.40 (4)	1.40			
Bond Angles (°)	**Experimental X-ray**	**6-31G(d,p)**	**Bond Angles (°)**	**Experimental X-ray**	**6-31G(d,p)**
C_2-N_1-C_{13}	115.2 (3)	116.7	C_5-C_{14}-C_{13}	124.0 (3)	121.5
N_1-C_2-N_3	123.4 (3)	124.3	C_5-C_{15}-C_6	117.4 (3)	116.6
N_1-C_2-S_{19}	122.6 (2)	119.5	C_5-C_{15}-C_{18}	122.1 (3)	122.0
N_3-C_2-S_{19}	114.0 (2)	116.2	C_6-C_{15}-C_{18}	120.4 (3)	121.4
C_2-N_3-C_4	123.1 (2)	121.1	C_6-C_{16}-C_7	119.0 (3)	118.9
N_3-C_4-C_{14}	114.8 (3)	113.8	C_6-C_{16}-C_{17}	121.5 (3)	121.4
N_3-C_4-O_{21}	120.0 (3)	114.7	C_7-C_{16}-C_{17}	119.4 (3)	119.8
C_{14}-C_4-O_{21}	125.2 (3)	131.5	C_{10}-C_{17}-C_{11}	119.8 (3)	118.9
C_{14}-C_5-C_{15}	109.0 (3)	110.7	C_{10}-C_{17}-C_{16}	120.4 (3)	120.0
C_{15}-C_5-C_{24}	110.7 (3)	108.4	C_{11}-C_{17}-C_{16}	119.8 (3)	121.0
C_{15}-C_6-C_{16}	117.7 (3)	116.5	C_{11}-C_{18}-N_{12}	113.4 (3)	114.8
C_{15}-C_6-O_{22}	120.9 (3)	122.5	C_{11}-C_{18}-C_{15}	123.3 (3)	123.1
C_{16}-C_6-O_{22}	121.3 (3)	120.9	N_{12}-C_{18}-C_{15}	123.2 (3)	122.1
C_8-C_7-C_{16}	119.9 (3)	120.1	C_2-S_{19}-C_{20}	101.5 (15)	104.5
C_7-C_8-C_9	120.7 (3)	120.1	C_5-C_{24}-C_{25}	121.9 (3)	118.8
C_8-C_9-C_{10}	120.1 (3)	120.0	C_5-C_{24}-C_{29}	120.2 (3)	121.6
C_9-C_{10}-C_{17}	119.5 (3)	120.0	C_{25}-C_{24}-C_{29}	117.8 (3)	119.6
C_{17}-C_{11}-C_{18}	117.0 (3)	115.8	C_{24}-C_{25}-C_{26}	121.4 (3)	120.7
C_{17}-C_{11}-O_{23}	123.9 (3)	123.9	C_{25}-C_{26}-C_{27}	119.9 (3)	118.6
C_{18}-C_{11}-O_{23}	119.1 (3)	120.2	C_{26}-C_{27}-C_{28}	119.1 (3)	121.8
C_{13}-N_{12}-C_{18}	120.6 (3)	118.9	C_{27}-C_{28}-C_{29}	119.9 (3)	118.4
N_1-C_{13}-N_{12}	114.2 (3)	115.0	C_{24}-C_{29}-C_{28}	121.9 (3)	121.0
N_1-C_{13}-C_{14}	126.1 (3)	123.6	C_{27}-O_{44}-C_{45}	117.9 (3)	117.8
N_{12}-C_{13}-C_{14}	119.7 (3)	121.4	O_{44}-C_{27}-C_{26}	124.5 (3)	123.2
C_4-C_{14}-C_5	118.8 (3)	118.0	O_{44}-C_{27}-C_{28}	116.4 (3)	116.0
C_4-C_{14}-C_{13}	117.2 (3)	120.4			

Table 3. *Cont.*

Dihedral Angles (°)	Experimental X-ray	6-31G(d,p)	Dihedral Angles (°)	Experimental X-ray	6-31G(d,p)
N_1-C_2-N_3-C_4	−0.7 (5)	1.3	C_{16}-C_{17}-C_{11}-C_{18}	−0.9 (5)	4.3
C_{13}-N_1-C_2-N_3	1.5 (5)	−1.3	C_{10}-C_{17}-C_{11}-C_{18}	177.8 (3)	−175.5
C_{13}-N_1-C_2-S_{19}	−178.9 (2)	179.2	C_6-C_{15}-C_{18}-N_{12}	179.5 (3)	174.5
S_{19}-C_2-N_3-C_4	179.7 (2)	−179.2	C_5-C_{15}-C_{18}-N_{12}	2.7 (5)	−6.1
C_2-N_3-C_4-O_{21}	176.3 (3)	−178.1	C_6-C_{15}-C_{18}-C_{11}	2.2 (5)	−5.2
C_2-N_3-C_4-C_{14}	−2.4 (5)	1.2	C_5-C_{15}-C_{18}-C_{11}	−174.6 (3)	174.2
O_{21}-C_4-C_{14}-C_{13}	−174.1 (3)	175.6	O_{24}-C_{11}-C_{18}-15	178.7 (3)	178.5
N_3-C_4-C_{14}-C_{13}	4.6 (5)	−3.6	C_{17}-C_{11}-C_{18}-15	1.1 (5)	−2.1
O_{21}-C_4-C_{14}-C_5	6.7 (5)	−5.8	O_{24}-C_{11}-C_{18}-N_{12}	1.2 (5)	−1.2
N_3-C_4-C_{14}-C_5	−174.7 (3)	175	C_{17}-C_{11}-C_{18}-N_{12}	−176.4 (3)	178.1
C_{13}-C_{14}-C_5-C_{15}	12.7 (5)	−18.2	C_{15}-C_{18}-N_{12}-C_{13}	5.7 (5)	−8.5
C_4-C_{14}-C_5-C_{15}	−168.1 (3)	163.1	C_{11}-C_{18}-N_{12}-C_{13}	−176.8 (3)	171.2
C_{13}-C_{14}-C_5-C_{24}	−109.7 (4)	102.8	C_2-N_1-C_{13}-C_{14}	1.1 (5)	−1.3
C_4-C_{14}-C_5-C_{24}	69.5 (4)	−75.9	C_2-N_1-C_{13}-N_{12}	−177.8 (3)	178.1
C_{14}-C_5-C_{15}-C_{18}	−10.8 (5)	18.4	C_4-C_{14}-C_{13}-N_1	−4.2 (5)	3.9
C_{24}-C_5-C_{15}-C_{18}	111.8 (4)	−104.7	C_5-C_{14}-C_{13}-N_1	174.9 (3)	−174.6
C_{14}-C_5-C_{15}-C_6	172.3 (3)	−162.1	C_4-C_{14}-C_{13}-N_{12}	174.7 (3)	−175.5
C_{24}-C_5-C_{15}-C_6	−65.1 (4)	74.8	C_5-C_{14}-C_{13}-N_{12}	−6.2 (5)	5.9
C_{18}-C_{15}-C_6-O_{22}	174.9 (3)	−168.9	C_{18}-N_{12}-C_{13}-N_1	175.1 (3)	−170.9
C_5-C_{15}-C_6-O_{22}	−8.1 (5)	11.6	C_{18}-N_{12}-C_{13}-C_{14}	−3.9 (5)	8.5
C_{18}-C_{15}-C_6-C_{16}	−5.5 (5)	10.1	N_1-C_2-S_{19}-C_{20}	−8.6 (3)	0.1
C_5-C_{15}-C_6-C_{16}	171.4 (3)	−169.4	N_3-C_2-S_{19}-C_{20}	171.1 (3)	−179.4
O_{22}-C_6-C_{16}-C_7	6.3 (5)	−8.4	C_{14}-C_5-C_{24}-C_{29}	71.1 (3)	−39.3
C_{15}-C_6-C_{16}-C_7	−173.2 (3)	172.6	C_{14}-C_5-C_{24}-C_{29}	−50.3 (4)	83.1
O_{22}-C_6-C_{16}-C_{17}	−174.7 (3)	171.1	C_{14}-C_5-C_{24}-C_{25}	−110.0 (3)	141.4
C_{15}-C_6-C_{16}-C_{17}	5.7 (5)	−7.9	C_{15}-C_5-C_{24}-C_{25}	128.7 (3)	−96.2
C_{17}-C_{16}-C_7-C_8	1.0 (5)	0.1	C_{25}-C_{24}-C_{29}-C_{28}	−0.1 (5)	−0.5
C_6-C_{16}-C_7-C_8	180.0 (3)	179.6	C_5-C_{24}-C_{29}-C_{28}	178.9 (3)	−179.8
C_{16}-C_3-C_3-C_9	0.4 (6)	−0.2	C_{24}-C_{29}-C_{28}-C_{27}	−0.5 (5)	0.1
C_7-C_8-C_9-C_{10}	−0.5 (6)	0.1	C_{29}-C_{28}-C_{27}-O_{44}	−178.6 (3)	179.9
C_8-C_9-C_{10}-C_{17}	−0.7 (5)	0.1	C_{29}-C_{28}-C_{27}-C_{26}	0.5 (5)	0.3
C_7-C_{16}-C_{17}-C_{10}	−2.2 (5)	0.2	O_{44}-C_{27}-C_{26}-C_{25}	179.1 (3)	180
C_6-C_{16}-C_{17}-C_{10}	178.8 (3)	−179.4	C_{35}-C_{27}-C_{26}-C_{25}	0.0 (4)	−0.4
C_7-C_{16}-C_{17}-C_{11}	176.5 (3)	−179.7	C_{27}-C_{26}-C_{25}-C_{24}	−0.6 (5)	0
C_6-C_{16}-C_{17}-C_{11}	−2.5 (5)	0.8	C_{29}-C_{24}-C_{25}-C_{26}	0.7 (4)	0.4
C_9-C_{10}-C_{17}-C_{16}	2.1 (5)	−0.3	C_{35}-C_{24}-C_{25}-C_{26}	−178.3 (3)	179.8
C_9-C_{10}-C_{17}-C_{11}	−176.6 (3)	179.6	C_{26}-C_{27}-O_{44}-C_{45}	9.9 (4)	−0.1
C_{16}-C_{17}-C_{11}-O_{24}	−178.4 (3)	−176.4	C_{28}-C_{27}-O_{44}-C_{45}	−171.0 (3)	179.9
C_{10}-C_{17}-C_{11}-O_{24}	0.3 (5)	3.8			

To study the vibrational characteristics and structural parameters of 5-(4-methoxyphenyl)-2-methylthio-5,12-dihydrobenzo[*g*]pyrimido[4,5-*b*]quinoline-4,6,11(3*H*)-trione **4c**, we performed a theoretical study at DFT level, which allows us to set the geometric and energetic parameters of the title compound. The optimized structure with B3LYP/6-31G(d,p) level is shown in Figure 2 [46–50]. The calculated geometric parameter (bond lengths, bond angles and dihedral angles) at same levels of calculation for title compound was compared with the experimental parameters, see Table 3, showing very good correlation.

The minimum point structures located on the potential surface scan (PES) for 5-(4-methoxyphenyl)-2-methylthio-5,12-dihydrobenzo[*g*]pyrimido[4,5-*b*]quinoline-4,6,11(3*H*)-trione **4c** was submitted for optimization using the B3LYP/6-31G(d,p) computational levels and theoretical approximations were performed in the gas phase. From the rotation of different groups, the minimum energy conformation and valuable structural information about compound are obtained. In order to reveal all possible conformational of the title compound, a detailed potential energy curve for τ1 (N_1-C_2-S_{19}-C_{20}), τ2 (C_{14}-C_5-C_{24}-C_{29}), and τ4 (C_{28}-C_{27}-O_{44}-C_{45}) dihedral angles was performed in steps of 10° from 0° to 360° and are described in Figure 4.

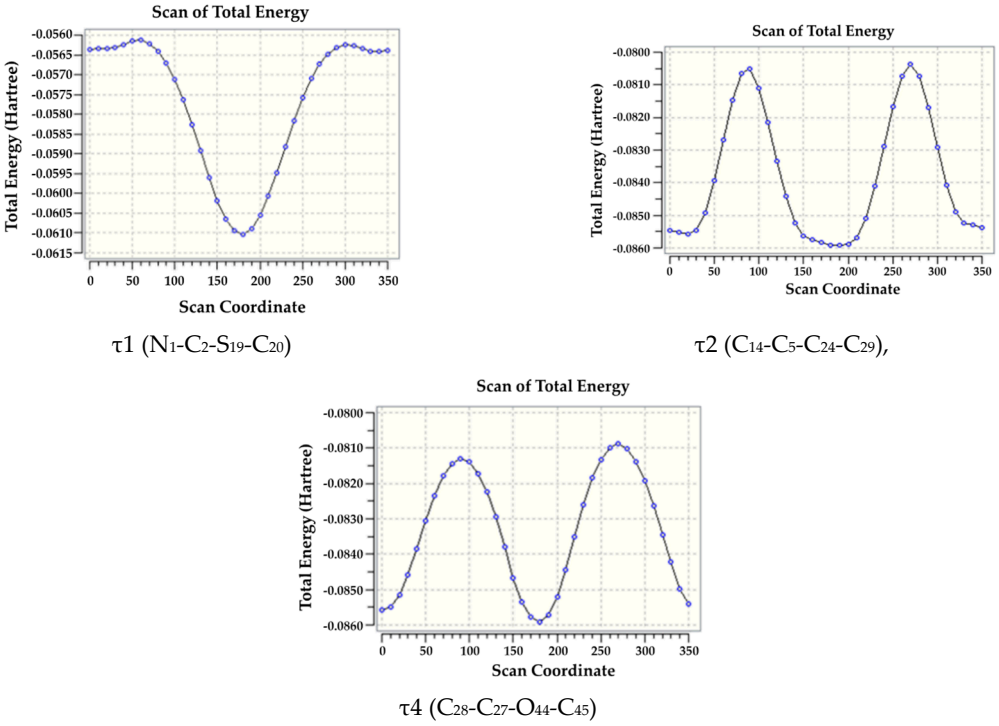

Figure 4. One-dimensional potential energy surface (PES) scan of the calculated energies vs. dihedral angles (τ) using DFT/B3LYP/6-31G(d,p) for 5-(4-methoxyphenyl)-2-methylthio-5,12-dihydrobenzo [*g*]pyrimido[4,5-*b*]quinoline-4,6,11(3*H*)-trione **4c**.

Structure of highest and lowest energy conformers for τ1, τ2 and τ4 dihedral angles and the computed values of these dihedral angles are given in Figure 4. The PES graphs are plotted using the conformation energies (kJ/mol) in Figure 5. The minimum energy curves for τ1 (N_1-C_2-S_{19}-C_{20}) dihedral angle were obtained at −0.78758° (−17.9 Kcal/mol), τ2 (C_{14}-C_5-C_{24}-C_{29}) −90.71251° (−18.0 Kcal/mol), and τ4 (C_{15}-C_5-C_{24}-C_{29}) at 178.04179° (−17.9 Kcal/mol) for B3LYP level.

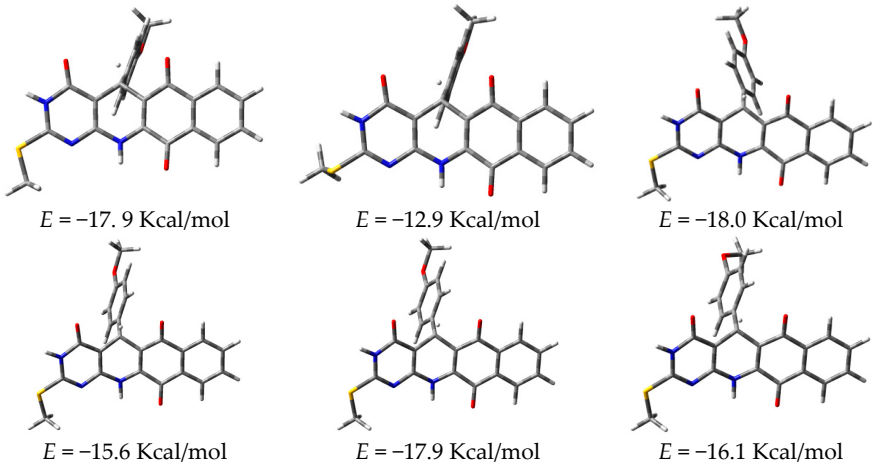

Figure 5. Highest and lowest energy conformations using DFT/B3LYP/6-31G(d,p) for 5-(4-methoxyphenyl)-2-methylthio-5,12-dihydrobenzo[*g*]pyrimido[4,5-*b*]quinoline-4,6,11(3*H*)-trione **4c**.

Vibrational spectral assignments (Table 4) were performed on the recorded FT-IR spectra, based on the theoretically predicted wavenumbers by DFT methods, using 6-31G(d,p) basis set [50]. The observed spectra are in good agreement with the simulated spectra.

Table 4. Fourier Transform infrared spectroscopy (FT-IR) Experimental and computed vibrational bands for compound **4c** and their assignments at B3LYP/6-31G(d,p) level.

υ	Experimental	Calculate		Assignment
		Un-Scaled	Scaled	
1	3272	3459	3334	N_{12}-H stretching
		3450	3325	N_3-H stretching
2	2841	3141	3027	O-CH_3 bending symmetric
		3127	3014	O-CH_3 stretching asymmetric
		3108	2996	S-CH_3 stretching asymmetric
		3039	2929	O-CH_3 stretching symmetric
		3018	2909	S-CH_3 stretching symmetric
3	1674	1851	1784	C_4=O_{21} stretching
4	1650	1822	1756	C_{11}=O_{23} stretching
5	1620	1811	1745	C_6=O_{22} stretching
6	1496	1495	1436	C=N stretching
7	1450	1467	1409	C=N stretching
8	1390	1350	1297	C-N stretching
9	1332	1185	1138	C-N stretching
10	1247	1126	1082	C-N stretching

The assignment of experimental vibrational bands to normal vibration modes is based on the comparison with related molecules and with results of the calculations obtained. We consider the B3LYP/6-31G(d,p) calculations because the scale factors used are well defined for this base set and also because the compared molecule was optimized at the same calculation level (0.961 ± 0.045) [51].

N-H vibrations

The bands at 3459 cm^{-1} and 3450 cm^{-1} are assigned to the symmetrical stretches of the N-H groups, N_{12} and N_3, respectively. These bands appear overlapping in the experimental spectrum at 3272 cm^{-1}.

C=O groups vibrations

The C=O stretches are observed as medium intensity bands at 1674 cm^{-1}, 1650 cm^{-1} and 1620 cm^{-1}. The DFT calculation gives the stretch wave number at 1784 cm^{-1} for stretching the C_4=O_{21} group, 1756 cm^{-1} for C_{11}=O_{23} and 1745 cm^{-1} for C_6=O_{22} after scaling. The difference between the calculated and experimental wave numbers can be attributed to the conjugation of C=O bonds to the phenyl ring, which is expected to decrease the wave numbers of the stretches.

C=N vibrations

Stretch bands C=N expected in the range of 1672–1566 cm^{-1}. For compound **4c**, the stretching mode C=N is assigned to 1496 cm^{-1} and 1450 cm^{-1} in FT-IR spectrum and theoretically at 1495 (1436) and 1467 (1409) cm^{-1}.

C-N vibrations

The C-N stretching vibrations are moderately to strongly in the 1275 ± 55 cm^{-1} region. According to reports in the literature, assign stretches of C-N are reported at 1184, 1367, and 1373 cm^{-1} for different compounds [52–54]. For compound **4c** the bands at 1390 and 1332 cm^{-1} are assigned to the C-N stretching modes and theoretically (DFT) at 1126 (1082), 1185 (1138) and 1350 (1297) cm^{-1}.

Two factors may be responsible for the discrepancies between the experimental and computed wavenumbers of the compound. The first is caused by the environment (gas and solid phase) and the second is because the experimental values are inharmonic wavenumbers while the calculated values are harmonic ones. Therefore, the calculated values are very close to experimental measures.

Natural bond orbital (NBO) analysis allows a detailed description of the electronic structure of compound **4c**, in terms of occupancy and composition of the group of NBOs Lewis (see Table 5) and not Lewis (see Table 6). 224 NBOs were calculated for this compound, representative NBOs are highlighted by finding three carbonyl-like bonds (C_4=O_{21}, C_6=O_{22}, C_{11}=O_{23}), a non-aromatic double bond (C_{15}=C_{18}), four heteroatom bonds (C_2-S_{19}, C_{27}-O_{44}, N_{12}-H_{31} and N_3-H_{30}) and solitary pairs of N and O (N_1, N_3, N_{12}, S_{19}, O_{21}, O_{22}, O_{23} and O_{44}) of the expected Lewis structure. For each of the molecular orbitals, the corresponding percentage of *s*, *p*, *d* character is included.

Table 5. Occupation of natural orbitals and hybrids for **4c** calculated by the DFT/B-3LYP/6-31G(d,p) method for the representative atoms.

Donor Lewis NBOs (Natural Bond Orbital)	Type	Electronic Density	Hybridization	Contribution of Natural Atomic Orbitals (%)			
					s	*p*	*d*
C_4-O_{21}	σ	1.99441	0.5952($sp^{2.01}$)C + 0.8036($sp^{1.43}$)O	C O	33.23 41.00	66.68 58.65	0.09 0.34
C_4-O_{21}	π	1.98431	0.5492 ($sp^{1.00}$)C + 0.835 ($sp^{1.00}$)O	C O	0.01 0.01	99.81 99.69	0.18 0.31
C_6-O_{22}	σ	1.99483	0.5895 ($sp^{2.31}$)C + 0.8078 ($sp^{1.38}$)O	C O	30.22 41.88	69.68 57.80	0.11 0.01
C_6-O_{22}	π	1.94776	0.5813 ($sp^{99.99}$)C + 0.8137 ($sp^{99.99}$)O	C O	0.01 0.02	99.84 99.67	0.14 0.31
C_{11}-O_{23}	σ	1.99525	0.5885 ($sp^{2.30}$)C + 0.8085 ($sp^{1.38}$)O	C O	30.26 41.89	69.63 57.79	0.11 0.32
C_{11}-O_{23}	π	1.95767	0.5756 ($sp^{1.00}$)C + 0.8177 ($sp^{1.00}$)O	C O	0.00 0.00	99.85 99.69	0.15 0.31
C_{15}-C_{18}	σ	1.97340	0.7021 ($sp^{1.83}$)C + 0.7121 ($sp^{1.51}$)C	C C	35.30 39.87	64.66 60.10	0.04 0.03
C_{15}-C_{18}	π	1.77932	0.7191 ($sp^{1.00}$)C + 0.6949 ($sp^{1.00}$)C	C C	0.00 0.00	99.94 99.95	0.06 0.05
C_2-S_{19}	σ	1.97646	0.7439 ($sp^{2.38}$)C + 0.6683 ($sp^{5.04}$)S	C S	29.51 16.44	70.38 82.84	0.10 0.73
C_{27}-O_{44}	σ	1.99168	0.5705 ($sp^{3.02}$)C + 0.8213 ($sp^{2.01}$)O	C O	24.82 33.17	74.97 66.76	0.21 0.07
N_{12}-H_{31}	σ	1.98356	0.8596 ($sp^{2.52}$)N + 0.5110 ($s^{99.89}$)H	N H	28.02 99.89	71.96 0.11	0.02
N_3-H_{30}	σ	1.98394	0.8551 ($sp^{2.61}$)N + 0.5184 ($s^{99.90}$)H	N H	27.68 99.90	72.29 0.10	0.02
N_1	LP [a] (1)	1.89271	$sp^{2.45}$	N	28.94	70.90	0.16
N_3	LP [a] (1)	1.61063	$p^{1.00}$	N	0.00	98.99	0.01
N_{12}	LP [a] (1)	1.73427	$sp^{90.58}$	N	1.09	98.89	0.01
O_{21}	LP [a] (1)	1.97642	$p^{1.00}$	O	58.92	41.03	0.04
O_{21}	LP [a] (2)	1.84939	$p^{99.99}$	O	0.03	99.73	0.24
O_{22}	LP [a] (1)	1.97885	$Sp^{0.72}$	O	58.07	41.88	0.04
O_{22}	LP [a] (2)	1.88965	$p^{1.00}$	O	0.00	99.80	0.20
O_{23}	LP [a] (1)	1.97850	$Sp^{0.72}$	O	58.02	41.93	0.05
O_{23}	LP [a] (2)	1.88503	$p^{1.00}$	O	0.05	99.74	0.20
O_{44}	LP [a] (1)	1.96389	$sp^{1.59}$	O	38.53	61.41	0.06
O_{44}	LP [a] (2)	1.84157	$p^{1.00}$	O	0.00	99.91	0.09
S_{19}	LP [a] (1)	1.98246	$Sp^{0.48}$	N	67.55	32.43	0.02
S_{19}	LP [a] (2)	1.82875	$p^{1.00}$	N	0.00	99.94	0.05

[a] Lone pair on natural Lewis structure.

Table 6. Occupation of natural bond orbitals (NBO) no Lewis and hybrids for **4c** calculated by the DFT/B-3LYP/6-31G(d,p) method for the representative atoms.

Acceptor not Lewis	Type	Electronic Density	Hybridization	Contribution of Natural Atomic Orbitals (%)			
					s	p	d
C_4-O_{21}	σ *	0.00892	0.8036 ($sp^{2.01}$)C − 0.5952 ($sp^{1.43}$)O	C O	33.23 41.00	66.68 58.65	0.09 0.34
C_4-O_{21}	π *	0.35268	0.8357 ($p^{1.00}$)C − 0.5492 ($p^{1.00}$)O	C O	0.01 0.01	99.81 99.69	0.18 0.31
C_6-O_{22}	σ *	0.00782	0.8078 ($sp^{2.31}$)C − 0.5895 ($sp^{1.38}$)O	C O	30.22 41.88	69.68 57.80	0.11 0.01
C_6-O_{22}	π *	0.20945	0.8137 ($p^{99.99}$)C − 0.5813 ($p^{99.99}$)O	C O	0.01 0.02	99.84 99.67	0.14 0.31
C_{11}-O_{23}	σ *	0.00754	0.8085 ($sp^{2.30}$)C − 0.5885 ($sp^{1.38}$)O	C O	30.26 41.89	69.63 57.79	0.11 0.32
C_{11}-O_{23}	π *	0.19366	0.8177 ($p^{1.00}$)C − 0.5756 ($p^{1.00}$)O	C O	0.00 0.00	99.85 99.69	0.15 0.310
C_{15}-C_{18}	σ *	0.02406	0.7121 ($sp^{1.83}$)C − 0.7021 ($sp^{1.51}$)C	C C	35.30 39.87	64.66 60.10	0.04 0.03
C_{15}-C_{18}	π *	0.24133	0.6949 ($p^{1.00}$)C − 0.7191 ($p^{1.00}$)C	C C	0.00 0.00	99.94 99.95	0.06 0.05
C_2-S_{19}	σ *	0.05230	0.6683 ($sp^{2.38}$)C − 0.7439 ($sp^{5.04}$)S	C S	29.51 16.44	70.38 82.84	0.10 0.73
C_{27}-O_{44}	σ	0.02955	0.8213 ($sp^{3.02}$)C − 0.5705 ($sp^{2.01}$)O	C O	24.82 33.17	74.97 66.76	0.21 0.07
N_{12}-H_{31}	σ *	0.02603	0.5110 ($sp^{2.52}$)N − 0.8596 ($s^{99.89}$)H	N H	28.02 99.89	71.96 0.11	0.02
N_3-H_{30}	σ	0.01822	0.5184 ($sp^{2.61}$)N + 0.8551 ($s^{99.90}$)H	N H	27.68 99.90	72.29 0.10	0.02

In Lewis type orbitals, as seen in Table 5, the σ bond (C_4-O_{21}) is formed from the $sp^{2.01}$ hybrid on carbon, mixture of *s* (33.23%) *p* (66.68%) *d* (0.09%); on the other hand, the π bond (C_4-O_{21}) is formed from the $sp^{1.00}$ hybrid on carbon and oxygen, mixture of *s* (0.01%) *p* (99.81%) *d* (0.18%); the electronic densities or maximum occupations calculated for σ (C_4-O_{21}), π (C_4-C_{21}), σ (C_6-C_{22}) and π (C_6-N_{22}) are 1.99441, 1.98431, 1.99483 and 1.94776, respectively. Therefore, these results allow to infer that these bonds are controlled by the character *p* of the hybrid orbitals.

The energy values E_2 for the interaction between the filled orbital *i* (donors) and the vacant orbital *j* (acceptors) or other molecular subsystem, calculated according to the theory of the second order perturbation, Equation (1), predicts the occurrence of delocalization or hyperconjugation [55,56]. The higher the value of E_2, the more intense the interaction between electron donors and the greater the degree of conjugation of the whole system [57].

$$E_2 = \Delta E_{ij} = q_i \frac{F(i,j)^2}{\varepsilon_j - \varepsilon_i} \quad (1)$$

q_i = Occupation or electronic density of the donor orbital.

E_i and E_j are the diagonal elements and $F(i, j)$ is the element of the Fock NBO diagonal matrix.

Therefore, we calculated the hyperconjugative interaction and density transfer of lone pair electron (LP) of the N_3 and N_{12} atoms to neighboring π antibonding orbitals. Similarly, the conjugation of carbonyl groups to neighboring atoms via π* → π*, see Table 7.

Table 7. Analysis perturbation theory second order in Fock matrix in NBO by level calculation B3LYP/6-31G (d,p) for compound **4c**.

Donor NBO (*i*)	Acceptor NBO (*j*)	E_2	E_j-E_i	*F(i,j)*
		Kcal/mol	**a.u**	**a.u**
LP N_3	π* N_1-C_2	65.72	0.26	0.116
LP N_3	π* C_4-O_{21}	44.57	0.30	0.104
LP N_{12}	π* C_{13}-C_{14}	41.73	0.30	0.101
LP N_{12}	π* C_{15}-C_{18}	39.97	0.30	0.101
π* C_4-O_{21}	π* C_{13}-C_{14}	256.96	0.01	0.080
π* C_6-O_{22}	π* C_{15}-C_{18}	94.72	0.02	0.076
π* C_{11}-O_{23}	π* C_{15}-C_{18}	41.82	0.04	0.075
π* C_{11}-O_{23}	π* C_{16}-C_{17}	76.69	0.03	0.075

In Table 7, the important contribution of LP N → π* interactions to the overall stability of the system is observed. Stability explained by the intramolecular electron transfer that occurs with these interactions. As evidence of this orbital phenomenon, it is the lowest electronic density on N3 and N12 compared to N1 (Table 6). The energy involved in the hyperconjugative interactions of the bonds between carbon and oxygen atoms of the carbonyl groups of molecule **4c**, give the most intense interactions and correspond to the highest degree of conjugation occurring in the α,β-unsaturated intramolecular system of aromatic ketones. π* (C_4-O_{21}) → π* (C_{13}-C_{14}), 257 kcal/mol; π* (C_6-O_{22}) → π* (C_{15}-C_{18}), 94.7 kcal/mol; π* (C_{11}-O_{23}) → π* (C_{15}-C_{18}), 41.8 kcal/mol; π* (C_{11}-O_{23}) → π* (C_{16}-C_{17}), 76.7 kcal/mol.

In the analysis of the nonlinear optical properties (NLO) for **4c**, the polarization of the molecule, induced by an external radiation field, it often resembles the generation of a dipole moment induced by an external electric field. Under the weak polarization condition, a Taylor serial development in the electric field components can be used to demonstrate the dipole interaction with the electric field of external radiation.

The first static hyperpolarizability (β_0) and its related properties (β, α_0 and $\Delta\alpha$) were calculated using the B3LYP/6-31G(d,p) level based on the finite field approach. The total static dipole moment μ, average polarizability α_0, anisotropy polarizability Δα and hyperpolarizability of first average β_0, using the components *x*, *y* and *z* is defined as:

$$\mu = \left(\mu_x^2 + \mu_y^2 + \mu_z^2\right)^{1/2} \quad (2)$$

$$\alpha_0 = \frac{1}{3}\left(\alpha_{xx} + \alpha_{yy} + \alpha_{zz}\right) \quad (3)$$

$$\Delta\alpha = 2^{-1/2}\left[\left(\alpha_{xx} - \alpha_{yy}\right)^2 + \left(\alpha_{yy} - \alpha_{zz}\right)^2 + \left(\alpha_{zz} - \alpha_{xx}\right)^2 + 6\alpha_{xz}^2\right]^{1/2} \quad (4)$$

First order hyperpolarizability is

$$\beta = \left(\beta_x^2 + \beta_y^2 + \beta_z^2\right)^{1/2} \quad (5)$$

where

$$\beta_y = \left(\beta_{yyy} + \beta_{yzz} + \beta_{yxx}\right) \quad (6)$$

$$\beta_z = \left(\beta_{zzz} + \beta_{zxx} + \beta_{zyy}\right) \quad (7)$$

$$\beta_x = \left(\beta_{xxx} + \beta_{xyy} + \beta_{xzz}\right) \quad (8)$$

$$\beta = \left[\left(\beta_{xxx} + \beta_{xyy} + \beta_{xzz}\right)^2 + \left(\beta_{yyy} + \beta_{yzz} + \beta_{yxx}\right)^2 + \left(\beta_{zzz} + \beta_{zxx} + \beta_{zyy}+\right)^2\right]^{1/2} \quad (9)$$

The polarizability and hyperpolarizability data are reported in atomic units (a.u), by Gaussian 09, reason why were converted into electrostatic units (esu) (α: 1 au = 0.1482 $\times$ 10^{-24} esu; β: 1 au = 8.639 $\times$ 10^{-33} esu). The mean polarization α_0 and total polarizability $\Delta\alpha$ for **4c** are 45.46 $\times$ 10^{-24} esu and 30.66 $\times$ 10^{-24} esu, respectively. The total molecular dipole momentum and first order hyperpolarizability are 1.88 Debye and 3768.07 $\times$ 10^{-33} esu, respectively, see Table 8.

Table 8. Electrical dipole moment, polarizability and first order hyperpolarizability of **4c** at the level DFT/B3LYP/6-31G(d,p).

Dipole Moment		Polarizability			First Order Hyperpolarizability		
Parameter	**D**	**Parameter**	**a.u**	**esu (10^{-24})**	**Parameter**	**a.u**	**esu (10^{-33})**
μ_x	−0.28	α_{xx}	373.29	55.26	β_{xxx}	1497.24	12941.0
μ_y	−1.34	α_{xy}	7.513	1.11	β_{xxy}	−165.57	−1431.10
μ_z	−1.28	α_{yy}	336.29	49.78	β_{xyy}	665.94	5755.80
μ_0	1.88	α_{xz}	12.913	1.91	β_{yyy}	−3426.60	−29,616.0
		α_{yz}	55.10	8.15	β_{xxz}	420.33	3633.0
		α_{zz}	211.86	31.36	β_{xyz}	72.03	622.60
		α_0	307.15	45.46	β_{yyz}	438.54	3790.30
		$\Delta\alpha$	207.15	30.66	β_{xzz}	20.44	176.73
					β_{yzz}	−87.92	−759.93
					β_{zzz}	−25.13	−217.26
					β_0 3768.07 $\times$ 10^{-33}		

These analysis frequently, are compared with the family of urea, as a reference for characterizing organic NLO materials [58,59]. The total dipole moment of the molecule is about 2.22 times lower than urea, and hyperpolarizability first order is 5.89 times higher than urea (μ and β for urea are 4.1775 Debye and 638.906 $\times$ 10^{-33} esu at the same calculation level). This result indicates the good non-linearity of the molecule.

The intramolecular charge transfer process, is determined by the separation E between the HOMO (highest energy occupied molecular orbital) and LUMO (lowest energy unoccupied molecular orbital) levels. Energy susceptible to adjust to λ in the range of visible light or tunable laser, by controllable variations due to the nature donor-acceptor of the groups. As an indirect method for determining potential NLO properties, the basal and excited state of a molecule is calculated and these results are used in the qualitative estimation of the efficiency of the intramolecular charge transfer process [60,61]. Which is related to the intramolecular electronic transfer in 5-arylaryl-2-methylthio-5,12-dihydrobenzo[*g*]pyrimido[4,5-*b*]quinoline-4,6,11(3*H*)-trione derivatives, the carbonyl groups being the acceptors of this charge transfer.

Finally, we compare the ground state energies of the optimized structures for 5-(4-methoxyphenyl)-2-methylthio-5,12-dihydrobenzo[*g*]pyrimido[4,5-*b*]quinoline-4,6,11(3*H*)-trione **4c** (obtained) and **5c** (Isomer angular uninsulated), with the aim to understand thermodynamic approach for the regiochemistry of the reaction shown Table 9. The calculated values show that 5c is thermodynamically more stable, however, is not formed. This suggests a kinetic control of the reaction.

Table 9. Ground state energies (enthalpy, Gibbs free energy and entropy) calculated for **4c** and **5c** compounds.

Thermodynamic Parameters	4c	5c
Enthalpy (H/a.u)	−549.949	−1181.96
Gibbs free energy (G/a.u)	−549.994	−1182.04
Entropy (S/cal mol^{-1} K^{-1})	93.941	172.531
ZEP (Zero-point energy) vibrational energy (Kcal/mol)	226.975	226.194
ZEP + electronic energy	−1749.749	−1749.758

4. Conclusions

To sum up, we can say this is an environmental friendly and straightforward methodology, to obtain by one-pot, three-component reactions the highly functionalized 5-aryl-2-methylthio-5,12-dihydrobenzo[*g*]pyrimido[4,5-*b*]quinoline-4,6,11(3*H*)-trione derivatives, with minimal waste formation, avoiding the use of toxic and/or hazardous solvents and reagents. The experimental results reveal a strong preference for the regioselective formation of linear four fused rings over the angular four fused rings. We have provided a theoretical/experimental comparative study to explain the regioselectivity that suggest a possible kinetic control in product formation.

The results of NBO analysis for compound **4c**, indicate that N12 is the bridge connecting the adjacent π systems, through orbital overlap *p* (LP N) and π* (C–C). Consequently, there is an intramolecular charge transfer originated by the movement of electronic clouds, from the donor to the acceptor (C=O groups), which is related to the nonlinear optical properties.

Supplementary Materials: The following are available online at http://www.mdpi.com/2076-3417/7/10/967/s1. ^{1}H NMR spectra and spectroscopic data for all of compounds reported here.

Acknowledgments: The authors thank "Centro de Instrumentación Científico-Técnica" Universidad de Jaén and the staff for data collection, and Consejería de Innovación, Ciencia y Empresa (Junta de Andalucía, Spain), Universidad del Valle, Universidad de Jaén, Universidad del Atlántico (For its 7th internal call FORTALECIMIENTO A GRUPOS DE INVESTIGACIÓN DE LA UNIVERSIDAD DEL ATLÁNTICO—CB36-FGI2016) and "Fundación para la Promoción de la Investigación y la Tecnología—Banco de la República" Proyecto No. 2.627, Convenio No. 201001 and COLCIENCIAS for financial support.

Author Contributions: J.T. and D.J.P. carried out the synthesis and spectroscopic characterization of synthesized compounds and monitored the experimental setup. A.P-G., A.O. implemented and carried out the computer studies. J.G. and J.Q. contributed with technical support and data analysis and interpretation. M.N. and J.C. carried out the X-ray diffraction analysis. All authors participated in drafting the manuscript, as well as reading and approving the final version of the manuscript.

Conflicts of Interest: The authors declare that they have no competing interests.

References

1. Lidström, P.; Tierney, J.; Wathey, B.; Westman, J. Microwave assisted organic synthesis—A Review. *Tetrahedron* **2001**, *57*, 9225–9283. [CrossRef]
2. Ashry, E.S.H.; Kassem, A.A. Account of microwave irradiation for accelerating organic reactions. *ARKIVOC* **2006**, *9*, 1–16. [CrossRef]
3. Martins, M.A.P.; Frizzo, C.P.; Moreira, D.N.; Buriol, L.; Machado, P. Solvent-Free Heterocyclic Synthesis. *Chem. Rev.* **2009**, *109*, 4140–4182. [CrossRef] [PubMed]
4. Strauss, C.R.; Varma, R.S. Microwaves in green and sustainable chemistry. *Top. Curr. Chem.* **2006**, *266*, 199–231. [CrossRef]
5. Quiroga, J.; Sánchez, N.; Acosta, P.; Insuasty, B.; Abonía, R. Microwave-assisted synthesis of fused pyrazolo[3,4-*b*]pyrazines by the reaction of ortho-aminonitrosopyrazoles and cyclic β-diketones. *Tetrahedron Lett.* **2012**, *53*, 3181–3187. [CrossRef]
6. Quiroga, J.; Trilleras, J.; Pantoja, D.; Abonía, R.; Insuasty, B.; Nogueras, M.; Cobo, J. Microwave-assisted synthesis of pyrazolo[3,4-*b*]pyridine-spirocycloalkanediones by three-component reaction of 5-aminopyrazole derivatives, paraformaldehyde and cyclic β-diketones. *Tetrahedron Lett.* **2010**, *51*, 4717–4719. [CrossRef]
7. Kappe, C.O. Controlled Microwave Heating in Modern Organic Synthesis. *Angew. Chem. Int. Ed.* **2004**, *43*, 6250–6284. [CrossRef] [PubMed]
8. Bougrin, K.; Loupy, A.; Soufiaoui, M. Microwave-assisted solvent-free heterocyclic synthesis. *J. Photochem. Photobiol. C Photochem. Rev.* **2005**, *6*, 139–167. [CrossRef]
9. Bariwal, J.B.; Trivedi, J.C.; Van der Eycken, E.V. Microwave Irradiation and Multicomponent Reactions. In *Synthesis of Heterocycles via Multicomponent Reactions II*; Orru, R., Ruijter, E., Eds.; Springer: Berlin/Heidelberg, Germany, 2010; Volume 25, pp. 169–230. ISBN 978-3-642-15455-3.

10. Dömling, A. Recent advances in isocyanide-based multicomponent chemistry. *Curr. Opin. Chem. Biol.* **2002**, *6*, 306–313. [CrossRef]
11. Hulme, C.; Gore, V. Multi-component reactions: Emerging chemistry in drug discovery from xylocain to crixivan. *Curr. Med. Chem.* **2003**, *10*, 51–80. [CrossRef] [PubMed]
12. Orru, R.V.A.; de Greef, M. Recent Advances in Solution-Phase Multicomponent Methodology for the Synthesis of Heterocyclic Compounds. *Synthesis* **2003**, *10*, 1471–1499. [CrossRef]
13. Quiroga, J.; Portillo, S.; Pérez, A.; Gálvez, J.; Abonía, R.; Insuasty, B. An efficient synthesis of pyrazolo[3,4-*b*]pyridine-4-spiroindolinones by a three-component reaction of 5-aminopyrazoles, isatin, and cyclic β-diketones. *Tetrahedron Lett.* **2011**, *52*, 2664–2666. [CrossRef]
14. Quiroga, J.; Portilla, J.; Serrano, H.; Abonía, R.; Insuasty, B.; Nogueras, M.; Cobo, J. Regioselective synthesis of fused benzopyrazolo[3,4-*b*]quinolines under solvent-free conditions. *Tetrahedron Lett.* **2007**, *48*, 1987–1990. [CrossRef]
15. Lang, G.; Pinkert, A.; Blunt, J.W.; Munro, M.H. Discorhabdin W, the first dimeric discorhabdin. *J. Nat. Prod.* **2005**, *68*, 1796–1798. [CrossRef] [PubMed]
16. Dömling, A. Recent Developments in Isocyanide Based Multicomponent Reactions in Applied Chemistry. *Chem. Rev.* **2006**, *106*, 17–89. [CrossRef] [PubMed]
17. Dömling, A.; Ugi, I. Multicomponent Reactions with Isocyanides. *Angew. Chem. Int. Ed.* **2000**, *39*, 3168–3220. [CrossRef]
18. Rawat, B.D.S. Antituberculosis drug research: A critical overview. *Med. Res. Rev.* **2013**, *33*, 693–764. [CrossRef]
19. Kaur, K.; Jain, M.; Reddy, R.P.; Jain, R. Quinolines and structurally related heterocycles as antimalarials. *Eur. J. Med. Chem.* **2010**, *45*, 3245–3264. [CrossRef] [PubMed]
20. Wiesner, J.; Ortmann, R.; Jomaa, H.; Schlitzer, M. New Antimalarial Drugs. *Angew. Chem. Int. Ed.* **2003**, *42*, 5274–5293. [CrossRef] [PubMed]
21. Mukherjee, S.; Pal, M. Quinolines: A new hope against inflammation. *Drug Discov. Today* **2013**, *18*, 389–398. [CrossRef] [PubMed]
22. Solomon, V.R.S.; Lee, H. Quinoline as a privileged scaffold in cancer drug discovery. *Curr. Med. Chem.* **2011**, *18*, 1488–1508. [CrossRef] [PubMed]
23. Quiroga, J.; Díaz, Y.; Bueno, J.; Insuasty, B.; Abonía, R.; Ortiz, A.; Nogueras, M.; Cobo, J. Microwave induced three-component synthesis and antimycobacterial activity of benzopyrazolo[3,4-*b*]quinolindiones. *Eur. J. Med. Chem.* **2014**, *74*, 216–224. [CrossRef] [PubMed]
24. Tao, Y.T.; Balasubramaniam, E.; Danel, A.; Jarosz, B.; Tomasik, P. Organic light-emitting diodes based on variously substituted pyrazoloquinolines as emitting material. *Chem. Mater.* **2001**, *13*, 1207–1212. [CrossRef]
25. Całus, S.; Gondek, E.; Danel, A.; Jarosz, B.; Pokładko, M.; Kityk, A.V. Electroluminescence of 6-R-1,3-diphenyl-1*H*-pyrazolo[3,4-*b*]quinoline-based organic light-emitting diodes (R=F, Br, Cl, CH_3, C_2H_3 and $N(C_6H_5)_2$). *Mater. Lett.* **2007**, *61*, 3292–3295. [CrossRef]
26. Kouznetsov, V.V.; Vargas Méndez, L.Y.; Meléndez Gómez, C.M. Recent progress in the synthesis of quinolones. *Curr. Org. Chem.* **2005**, *9*, 141–161. [CrossRef]
27. Trilleras, J.; López, L.G.; Pacheco, D.J.; Quiroga, J.; Nogueras, M.; De la Torre, J.M.; Cobo, J. Efficient Microwave-Assisted Synthesis of 5-Deazaflavine Derivatives. *Molecules* **2010**, *15*, 7227–7234. [CrossRef] [PubMed]
28. Trilleras, J.; López, L.G.; Cobo, J.; Glidewell, C. 10-Benzyl-4-oxo-2,3,4,10-tetrahydropyrimido[4,5-*b*]quinolin-2-iminium chloride sesquihydrate: A polarized electronic structure within a complex hydrogen-bonded sheet structure. *Acta Crystallogr. Sect. C* **2010**, *66*, 469–472. [CrossRef] [PubMed]
29. Quiroga, J.; Trilleras, J.; Insuasty, B.; Abonía, R.; Nogueras, M.; Marchal, A.; Cobo, J. A straightforward synthesis of pyrimido[4,5-*b*]quinoline derivatives assisted by microwave irradiation. *Tetrahedron Lett.* **2010**, *51*, 1107–1109. [CrossRef]
30. Ivanov, I.; Nikolava, S.; Aladjov, D.; Stefanova, I.; Zagorchev, P. Synthesis and Contractile Activity of Substituted 1,2,3,4-Tetrahydroisoquinolines. *Molecules* **2011**, *16*, 7019–7042. [CrossRef] [PubMed]
31. Niralwad, K.S.; Shingate, B.B. Microwave-assisted one-pot synthesis of octahydroquinazolinone derivatives using ammonium metavanadate under solvent-free condition. *Tetrahedron Lett.* **2010**, *51*, 3616–3618. [CrossRef]

32. Stöckigt, J.; Antonchick, A.P.; Wu, F.; Waldmann, H. The Pictet–Spengler Reaction in Nature and in Organic Chemistry. *Angew. Chem. Int. Ed.* **2011**, *50*, 8538–8564. [CrossRef] [PubMed]
33. Hasssaneen, H.M.; Hassaneen, H.M.E.; Mohammed, Y.S. Reactivity of 1-methylisoquinoline synthesis of pyrazolyl triazoloisoquinoline and thiadiazolyl isoquinoline derivatives. *Nat. Sci.* **2011**, *3*, 651–660. [CrossRef]
34. Aknin, K.; Desbène-Finck, S.; Helissey, P.; Giorgi-Renault, S. A new synthetic approach to functionalize pyrimido[4,5-*b*]quinoline-2,4(1*H*,3*H*)-diones via a three-component one-pot reaction. *Mol. Divers.* **2010**, *14*, 123–130. [CrossRef] [PubMed]
35. Quiroga, J.; Insuasty, B.; Insuasty, H.; Abonía, R.; Ortiz, A.; Sánchez, A.; Nogueras, M. Reactions of 6-aminopyrimidines with 2-dimethylaminomethylenetetralone. Regiospecific Synthesis of 5,6-Dihydrobenzo[*h*]pyrimido[4,5-*b*]quinolones. *J. Heterocycl. Chem.* **2001**, *38*, 339–341. [CrossRef]
36. Quiroga, J.; Hormaza, A.; Insuasty, B.; Ortíz, A.; Sánchez, A.; Nogueras, M. Synthesis of pyrimido[4,5-*b*]quinolines in the reaction of 6-aminopyrimidines with dimedone and benzaldehydes. *J. Heterocycl. Chem.* **1998**, *35*, 231–233. [CrossRef]
37. Shi, D.-Q.; Niu, L.-H.; Yao, H.; Jiang, H. An efficient synthesis of pyrimido[4,5-*b*]quinoline derivatives via three-component reaction in aqueous media. *J. Heterocycl. Chem.* **2009**, *46*, 237–242. [CrossRef]
38. Chen, Y.; Wu, S.; Tu, S.; Shi, F.; Li, C. An efficient synthesis of new benzo[1′,2′:6,7]quinolino[2,3-d]-pyrimidine derivatives via three-component microwave-assisted reaction. *J. Heterocycl. Chem.* **2008**, *45*, 1243–1246. [CrossRef]
39. Azizian, J.; Delbari, A.S.; Yadollahzadeh, K. One-Pot, Three-Component Synthesis of Pyrimido[4,5-*b*]quinoline-tetraone Derivatives in Water. *Synth. Commun.* **2014**, *44*, 3277–3286. [CrossRef]
40. Chen, C.; Zhu, X.; Wu, Y.; Sun, H.; Zhang, G.; Zhang, W.; Gao, Z. 5-Sulfosalicylic acid catalyzed direct Mannich reaction in pure water. *J. Mol. Catal. A Chem.* **2014**, *395*, 124–127. [CrossRef]
41. Wu, Y.; Chen, C.; Jia, G.; Zhu, X.; Sun, H.; Zhang, G.; Zhang, W.; Gao, Z. Salicylato Titanocene Complexes as Cooperative Organometallic Lewis Acid and Brønsted Acid Catalysts for Three-Component Mannich Reactions. *Chem. Eur. J.* **2014**, *20*, 8530–8535. [CrossRef] [PubMed]
42. Frisch, M.J.; Trucks, G.W.; Schlegel, H.B.; Scuseria, G.E.; Robb, M.A.; Cheeseman, J.R.; Scalmani, G.; Barone, V.; Mennucci, B.; Petersson, G.A.; et al. *Gaussian 09*, version A.02; Gaussian, Inc.: Wallingford, CT, USA, 2009.
43. Gang, L.; Hankui, W.; Zhiyong, W.; Xianli, W. One-Pot Three-Component Mannich-Type Reaction Catalyzed by Trifluoromethanesulfonic Acid in Water. *Kinet Catal.* **2011**, *52*, 89–93. [CrossRef]
44. Zheng, X.; Qian, Y.B.; Wang, Y. 2-Pyrrolidinecarboxylic Acid Ionic Liquid as a Highly Efficient Organocatalyst for the Asymmetric One-Pot Mannich Reaction. *Eur. J. Org. Chem.* **2010**, 515–522. [CrossRef]
45. Castillo, Y.A.; Zapata, L.F.; Trilleras, J.; Cobo, J.; Glidewell, C. (5RS)-5-(4-Methoxyphenyl)-2-(methylsulfanyl) benzo[*g*]pyrimido[4,5-*b*]quinoline-4,6,11(3H,5H,12H)-trione, with Z′=3, forms a three-dimensional hydrogen-bonded framework containing five types of hydrogen bond. *Acta Cryst. Sect. C* **2014**, *70*, 50–54. [CrossRef] [PubMed]
46. Tirado-Rives, J.; Jorgensen, W.L. Performance of B3LYP Density Functional Methods for a Large Set of Organic Molecules. *J. Chem. Theory Comput.* **2008**, *4*, 297–306. [CrossRef] [PubMed]
47. Torres, E.; DiLabio, G.A. A (Nearly) Universally Applicable Method for Modeling Noncovalent Interactions Using B3LYP. *J. Phys. Chem. Lett.* **2012**, *3*, 1738–1744. [CrossRef] [PubMed]
48. Krishnakumar, V.; Mathammal, R. Density functional and experimental studies on the FT-IR and FT-Raman spectra and structure of benzoic acid and 3,5-dichloro salicylic acid. *J. Raman Spectrosc.* **2009**, *40*, 264–271. [CrossRef]
49. El-Azhary, A.A. Comparison between Optimized Geometries and Vibrational Frequencies Calculated by the DFT Methods. *J. Phys. Chem.* **1996**, *100*, 15056–15063. [CrossRef]
50. Avci, D.; Atalay, Y. Theoretical analysis of vibrational spectra and scaling-factor of 2-aryl-1,3,4-oxadiazole derivatives. *Int. J. Quantum Chem.* **2009**, *109*, 328–341. [CrossRef]
51. Computational Chemistry Comparison and Benchmark DataBase. Release 18 (October 2016) Standard Reference Database 101. National Institute of Standards and Technology. Available online: http://cccbdb.nist.gov/energy1x.asp (accessed on 23 September 2015).
52. Manivanna, S.; Dhanuskodi, S. Growth and characterization of a new organic nonlinear optical crystal: Semicarbazone of p-dimethylamino benzaldehyde. *J. Cryst. Growth* **2003**, *257*, 305–308. [CrossRef]

53. Trzesowska, A. P-Dimethylaminobenzaldehyde semicarbazone: The bonding abilities of imine nitrogen atom. *J. Mol. Struct.* **2009**, *917*, 125–132. [CrossRef]
54. An, B.L.; Gong, M.L.; Cheah, K.W.; Wong, W.K.; Zhang, J.M. Synthesis, structure and photoluminescence of novel lanthanide (Tb (III), Gd (III)) complexes with 6-diphenylamine carbonyl 2-pyridine carboxylate. *J. Alloys Compd.* **2004**, *368*, 326–332. [CrossRef]
55. Balachandran, V.; Karunakaran, V. Quantum mechanical study of the structure and vibrational spectroscopic (FT-IR and FT-Raman), first-order hyperpolarizability, NBO and HOMO−LUMO studies of 4-bromo-3-nitroanisole. *Spectrochim. Acta Part A* **2013**, *106*, 284–298. [CrossRef] [PubMed]
56. Yang, Y.; Zhang, W.; Gao, X. Blue-shifted and red-shifted hydrogen bonds: Theoretical study of the $CH_3CHO\cdots HNO$ complexes. *Int. J. Quantum Chem.* **2006**, *106*, 1199–1207. [CrossRef]
57. Tavakkoli, H.; Farhadipour, A. Mononuclear gallium (III) complexes based on salicylaldoximes: Theoretical study of structures, topological and NBO analysis of hydrogen bonding interactions involving O–H···O bonds. *Arab. J. Chem.* **2016**, *9*, S361–S372. [CrossRef]
58. Jagadeesha, M.R.; Kumar, H.M.S.; Kumari, R.A. Crystal growth and characterization of a new NLO crystal: Urea 2-furoic acid. *Optik* **2015**, *126*, 4014–4018. [CrossRef]
59. Luo, S.J.; Yang, J.T.; Du, W.F.; Laref, A. Mechanism of Linear and Nonlinear Optical Properties of the Urea Crystal Family. *J. Phys. Chem. A* **2011**, *115*, 5192–5200. [CrossRef] [PubMed]
60. Marañón-Ruiz, V.F.; Rizo de la Torre, L.D.C.; Chiu-Zarate, R. Caracterización de las propiedades ópticas de Betacianinas y Betaxantinas por espectroscopía Uv-Vis y barrido en Z. *Superf. Vacio* **2011**, *24*, 113–120.
61. Hrobarik, P.; Zahradnik, P.; Fabian, W.M.F. Computational design of benzothiazole-derived push–pull dyes with high molecular quadratic hyperpolarizabilities. *Phys. Chem. Chem. Phys.* **2004**, *6*, 495–502. [CrossRef]